

JPRS-UEQ-91-008
27 JUNE 1991

Foreign
Broadcast
Information
Service



A N N I V E R S A R Y
1 9 4 1 - 1 9 9 1

JPRS Report

Science & Technology

***USSR: Engineering &
Equipment***

19980116 222

DTIC QUALITY INSPECTED 2

REPRODUCED BY
U.S. DEPARTMENT OF COMMERCE
NATIONAL TECHNICAL INFORMATION SERVICE
SPRINGFIELD, VA. 22161

DISTRIBUTION STATEMENT A

Approved for public release;
Distribution Unlimited

Science & Technology

USSR: Engineering & Equipment

JPRS-UEQ-91-008

CONTENTS

27 June 1991

Optics, High Energy Devices

| | |
|---|---|
| Rasters Based on Hadamard Matrices for Oscillation Mode [V.V. Afanasyev, V.B. Shlishevskiy; <i>IZVESTIYA VYSSHIKH UCHEBNYKH ZAVEDENIY: PRIBOROSTROYENIYE, Dec 90</i>] | 1 |
| Measurement Data Processing Method and Equipment for Surface Shape Inspection [M.A. Kropotkin, A.L. Melkonyan; <i>IZVESTIYA VYSSHIKH UCHEBNYKH ZAVEDENIY: PRIBOROSTROYENIYE, Dec 90</i>] | 1 |
| Peculiarities of Reproduction Tomographic Images With Varifocal Mirror Objective [G.V. Mamchev; <i>IZVESTIYA VYSSHIKH UCHEBNYKH ZAVEDENIY: PRIBOROSTROYENIYE, Dec 90</i>] | 1 |
| Processing Optical Measurements Data in Multiposition Small-Base Observation System [A.I. Daugavet, Ye.V. Postnikov; <i>IZVESTIYA VYSSHIKH UCHEBNYKH ZAVEDENIY: PRIBOROSTROYENIYE, Dec 90</i>] | 2 |
| Increasing Corrective Power of Spherochromatic Aberration Compensator and Its Use in High-Speed Photographic Cameras With Scanning by Mirror [A.V. Belinskiy, I.V. Petrochenko, et al.; <i>IZVESTIYA VYSSHIKH UCHEBNYKH ZAVEDENIY: PRIBOROSTROYENIYE, Dec 90</i>] | 2 |
| Mirror Compensator of Image Rotation [M.V. Dorofeyeva; <i>IZVESTIYA VYSSHIKH UCHEBNYKH ZAVEDENIY: PRIBOROSTROYENIYE, Dec 90</i>] | 2 |
| Design of Mirror Objectives With Planoidal (Nearly Plane) Surfaces [G.I. Tsukanova; <i>IZVESTIYA VYSSHIKH UCHEBNYKH ZAVEDENIY: PRIBOROSTROYENIYE, Dec 90</i>] | 3 |

Non-Nuclear Energy

| | |
|--|---|
| On Problem of Evaluating Wind Energy Potential of Armenia [A.A. Mardzhanyan, G.S. Petrosyan, et al.; <i>IZVESTIYA AKADEMII NAUK ARMYANSKOY SSR: SERIYA TEKHNIЧЕСКИХ НАУК, No 4 90</i>] | 4 |
| The USSR Coal Industry in 1990 [UGOL UKRAINY, No 4, 91] | 5 |

Mechanics of Gases, Liquids, Solids

| | |
|---|----|
| Dynamics of Asymmetric Interaction Involving Body of Revolution and Rigid Barrier [I.Ye. Khorev, N.T. Yugov; <i>PRIKLADNAYA MEKHANIKA, Nov 90</i>] | 10 |
| Experimental Study of Dynamic Deformation of Hollow Elastic Cylindrical Shells Immersed in Water and Vacuumized [I.I. Anikye, M.I. Mikhaylova, et al.; <i>PRIKLADNAYA MEKHANIKA, Nov 90</i>] | 10 |
| Nonlinear Deformation of Cylindrical Shell by Local Thermal Shock [N.I. Obodan, N.B. Makarenko; <i>PRIKLADNAYA MEKHANIKA, Nov 90</i>] | 10 |
| Transient Processes in Electrically Excited Multilayer Piezoceramic Stack [A.E. Babayev, V.G. Savin; <i>PRIKLADNAYA MEKHANIKA, Nov 90</i>] | 11 |
| Nonaxisymmetric Stressed and Strained State of Anisotropic Multilayer Shells of Revolution [G.M. Kulikov; <i>PRIKLADNAYA MEKHANIKA, Nov 90</i>] | 11 |
| Dispersion Equations for Electroelastic Shear Waves in Multilayer Media With Periodic Structure [L.P. Zinchuk, A.N. Podlipenets; <i>PRIKLADNAYA MEKHANIKA, Nov 90</i>] | 11 |
| Use of Asymptotic Method for Analysis of Finite-Amplitude Vibrations of Flat Shells [N.I. Zhinzher, V.Ye. Khromatov; <i>PRIKLADNAYA MEKHANIKA, Nov 90</i>] | 12 |
| Forced Longitudinal Oscillations of Long Pipe Containing Liquid [V.S. Tikhonov, V.I. Komissarenko, et al.; <i>PRIKLADNAYA MEKHANIKA, Nov 90</i>] | 12 |
| Propagation of Shear Waves Through Nonlinearly Elastic Body [V.I. Yerofeyev, I.G. Raskin; <i>PRIKLADNAYA MEKHANIKA, Jan 91</i>] | 12 |
| Longitudinal Damped Vibrations of Plates [A.S. Kosmodamianskiy, M.N. Gofman; <i>PRIKLADNAYA MEKHANIKA, Jan 91</i>] | 13 |
| Action of Acoustic Wave on Set of Two Parallel Circular Cylinders in Ideal Fluid [A.P. Zhuk; <i>PRIKLADNAYA MEKHANIKA, Jan 91</i>] | 13 |

| | |
|---|----|
| Resonance Dynamics of Vessel With Liquid Mounted on Vibration Dampers [G.N. Puchka, V.V. Kholopova; PRIKLADNAYA MEKHANIK, Jan 91] | 14 |
| Stability Theory for Motion of Triple-Unit Vehicles on Tires [L.G. Lobas, V.P. Sakhno, et al.; PRIKLADNAYA MEKHANIK, Jan 91] | 14 |
| Vibrations of Reflector Antenna Shells Under Vibratory Excitation [V.S. Gudramovich, N.G. Baranov, et al.; PRIKLADNAYA MEKHANIK, Jan 91] | 15 |
| Design of Viscoelastic Thin-Walled Shells Considering Their Damageability [Ya.A. Eyubov; PRIKLADNAYA MEKHANIK, Jan 91] | 15 |
| Use of Acoustoelasticity Theory of Rayleigh Surface Waves for Determination of Stresses in Solid Bodies [A.A. Chernoochenko, F.G. Makhort, et al.; PRIKLADNAYA MEKHANIK, Jan 91] | 15 |
| Stressed and Strained State of Half-Space Due to Translatory Motion and Rotation of Partly Embedded Rigid Ball Partly [I.K. Senchenkov, V.G. Savchenko, et al.; PRIKLADNAYA MEKHANIK, Jan 91] | 16 |
| Stressed State of Noncircular Thick-Walled Cylinders Depending on Indicators of Load Nonuniformity Along Generatrix and Directrix [Ya.M. Grigorenko, G.G. Vlaykov, et al.; PRIKLADNAYA MEKHANIK, Mar 91] | 16 |
| Solution of Problems Pertaining to Parametric Vibrations of Shells of Revolution by Method of Finite Elements [A.T. Vasilenko, S.S. Kokoshin, et al.; PRIKLADNAYA MEKHANIK, Mar 91] | 17 |
| Axisymmetric Problem of Impact of Solid Body against Thin Membrane Floating on Compressible Fluid Half-Space [V.D. Kubenko, V.V. Gavrilenko; PRIKLADNAYA MEKHANIK, Mar 91] | 17 |
| Viscoelastic State of Cylindrical Triple-Layer Shell Under Pulsed Heat or Force Load [E.I. Starovoytov, S.A. Vorobyev; PRIKLADNAYA MEKHANIK, Mar 91] | 18 |
| Elastic Displacements Vector of Thin Spherical Shell [V.A. Merkulov; PRIKLADNAYA MEKHANIK, Mar 91] | 18 |
| Numerical Analysis of Statics of Smooth and Discretely Reinforced Shells Under Combined Flexural and Axial Load [V.P. Maksimenko, N.V. Kovalchuk; PRIKLADNAYA MEKHANIK, Mar 91] | 19 |
| Supercritical Deformation of Real Cylindrical Shells Under External Pressure and Estimation of Their Stability [A.Yu. Yevkin, V.L. Krasovskiy; PRIKLADNAYA MEKHANIK, Mar 91] | 19 |
| Vibrations of Triple-Layer Plate of Finite Dimensions in Contact With Liquid [S.N. Beshenkov, T.D. Volkova; PRIKLADNAYA MEKHANIK, Mar 91] | 20 |
| Interaction of Acoustic Wave and Two Parallel Cylinders in Viscous Fluid [A.P. Zhuk; PRIKLADNAYA MEKHANIK, Mar 91] | 20 |
| Design of Framed Shells of Intricate Shapes for Internal Pressure Load [V.V. Kuznetsov, Yu.V. Soynikov; PRIKLADNAYA MEKHANIK, Mar 91] | 21 |
| Experimental Stability Study of Nonconservative Systems [M.Kh. Mullagulov; PRIKLADNAYA MEKHANIK, Mar 91] | 21 |

Industrial Technology, Planning, Productivity

| | |
|---|----|
| Design of Closed-Loop for Control of Robot With Torque Motors [A.F. Timofeyev, V.A. Baykalov, et al.; IZVESTIYA VYSSHIKH UCHEBNYKH ZAVEDENIY: PRIBOROSTROYENIYE, Dec 90] | 22 |
|---|----|

Rasters Based on Hadamard Matrices for Oscillation Mode

917F0163G Leningrad IZVESTIYA VYSSHIKH
UCHEBNIKH ZAVEDENIY: PRIBOROSTROYENIYE
in Russian No 12, Dec 90 pp 74-77

[Article by V.V. Afanasyev and V.B. Shlishevskiy,
Novosibirsk Institute of Geodetic, Aerial Photography,
and Cartography Engineers]

UDC 681.782.5

[Abstract] Use of rasters based on Hadamard matrices for spectrometers operating with selective modulation of the luminous flux in the oscillation mode is considered, the essential requirement being that their autocorrelation function have no maxima besides those characterizing the dependence on the number of raster element. While such rasters constructed for selective modulation in the switching mode already have this property, their structure needs to be modified so as to make accurate quantitative measurements in the stable and reliable oscillation mode feasible. Such a modification involves transposition of rows and columns in the original matrix, which will not break its orthogonality. Sifting all possible transposition variants becomes simple when used is made of the relation $H_2 = PH_1Q$, which represents the equivalence of two Hadamard matrices H_1 and H_2 . The monomial transposition matrices have each only one nonzero element in each row and in each column: a +1 or a -1, representing respectively transparent and opaque elements of the raster. Figures 2; references 5.

Measurement Data Processing Method and Equipment for Surface Shape Inspection

917F0163F Leningrad IZVESTIYA VYSSHIKH
UCHEBNIKH ZAVEDENIY:
PRIBOROSTROYENIYE No 12, Dec 90 pp 69-74

[Article by M.A. Kropotkin (deceased), A.L. Melkonyan,
and M.B. Stolbov, Leningrad Institute of Electrical Engineering imeni V.I. Ulyanov (Lenin)]

UDC 621.375

[Abstract] One noteworthy application for optoelectronic systems is monitoring deformations of intricate surfaces in the product quality control process. Such a system consists essentially of an optoelectronic transducer, a device for orienting the inspection object relative to it, a scanner, a recording instrument, and an interface to a computer. Scanning and recording can be combined by using a photodiode matrix or a photoelectric charge-coupled-device matrix. The operation of such a system is demonstrated on inspection of axisymmetric objects such as reflector antennas, paraboloids of revolution. The processing of measurement data depends on the description of the inspected surface in terms of approximating functions, Zernicke polynomials

having been selected for monitoring large deformations. The measurement procedure is accordingly determined by the parameters of the surface model which need to be estimated. The algorithm of calculating surface deformations at points on the surface takes into account the distance from scanner to inspected surface. It includes correction of the object position relative to the transducer, either for compensation of the positioning error or for minimization of the effect of surface deformations on the antenna performance characteristics. Such a correction involves determination of the approximating surface, which is done by variation of the object position parameters B^T = unordered set: $\delta z, \delta x, \delta y, \delta \psi^x, \delta \psi^y$ (linear displacements in x, y, and z directions, angular displacements by rotation about X and Y axes). The magnitudes of these variations are determined from the measurement data by the method of least squares and the effect of each of these displacements on the deviation of the object surface along the normal to it is described in terms of respective influencing functions. Compensation of homologous surface deformations is considered, the necessary number of inspection points being established by expansion of the influencing functions into Zernicke polynomial series and compensation then being achieved by minimization of residual phase distortions in the antenna aperture. From the measurement data can also be determined the change in antenna performance parameters, gain and radiation pattern, owing to compensation of homologous surface distortions. Figures 1; references 3.

Peculiarities of Reproduction Tomographic Images With Varifocal Mirror Objective

917F0163B Leningrad IZVESTIYA VYSSHIKH
UCHEBNIKH ZAVEDENIY: PRIBOROSTROYENIYE
in Russian No 12, Dec 90 pp 52-56

[G.V. Mamchev, Novosibirsk Institute of Electrical Communications Engineering]

UDC 621.397.13:681.3.04

[Abstract] Reproduction of three-dimensional multiplanar tomographic images in medical practice is considered, use of a varifocal parabolic mirror objective having been proposed for computer-aided tomography. The process involves spatial superposition of two-dimensional images depicting each another parallel section of the object and to be seen one behind the other in space in the following sequence: 1, 2, ..., n-1, n, n-1, n-1, ..., 3, 2, 1, 2, ..., n, ... (n - number of synthesized images of parallel sections). One possible version of a varifocal mirror objective is an aluminum-coated mylar film spread over a loudspeaker and splitting incident light by reflecting one part of it at a 90° angle onto the screen of the cathode-ray tube while transmitting the other part straight through. The design problem of determining that number n of images is tackled by taking into account the characteristics of binocular vision. The

depth of vision threshold needs to be determined accurately on a statistical basis, a special experiment involving reception of televised images having for this purpose been performed in which the background luminance was varied over the 2-40 cd/m² range and the signal-to-noise ratio was varied over the 6-40 dB range. The design procedure is demonstrated on such a mirror objective for a 61LK2B kinescope: aperture diameter of spherical mirror 2R = 610 mm equal to kinescope screen size (diagonal dimension), distance from kinescope to mirror in its central position a = 500 mm, mirror film vibrating at a frequency $f_a = 50$ Hz with a maximum amplitude $\Delta_{\max} = 1-2$ mm, $n = 7-14$, frequency of vertical scan $f_v = n f_a = 350-700$ Hz, number of resolution lines $z = 625$, frequency of line scan $f_z = 19-438$ kHz. Figures 2; references 3.

Processing Optical Measurements Data in Multiposition Small-Base Observation System

917F0163D Leningrad IZVESTIYA VYSSHIKH UCHEBNIKH ZAVEDENIY: PRIBOROSTROYENIYE in Russian No 12, Dec 90 pp 60-65

[Article by A.I. Daugavet and Ye.V. Postnikov, Leningrad Institute of Electrical Engineering imeni V.I. Ulyanov (Lenin)]

UDC 621.391

[Abstract] The performance of an optical multiposition observation system for determining the angular coordinates of remote objects is analyzed for accuracy of their estimates, that accuracy depending largely on the length of the "measurement base". Systems with space diversity of at least two stations of the same type are considered for estimating the radius- vector of a point in space on the basis of the readings of its coordinates. The covariant estimation matrix is constructed for such a system and the Rao-Kramer inequality is applied here, assuming a Mises distribution of the random quantity $\zeta_i = (\omega_i, \bar{\omega}_i^*)$ on the $[-1, 1]$ segment ($\bar{\omega}_i$ - readings of real direction angles ω_i^* , vectors ω_i - random points on a unit sphere) so that its probability density function is $p(z) = Ae^{az}$. The results indicate that such a system must have a measurement base sufficiently long to make the angles between the directions from its stations to the target at least one order of magnitude larger than the angle measurement errors. References 3.

Increasing Corrective Power of Spherochromatic Aberration Compensator and Its Use in High-Speed Photographic Cameras With Scanning by Mirror

917F0163C Leningrad IZVESTIYA VYSSHIKH UCHEBNIKH ZAVEDENIY: PRIBOROSTROYENIYE in Russian No 12, Dec 90 pp 56-60

[Article by A.V. Belinskiy, I.V. Petrochenko, and A.V. Plokhov, Moscow Institute of Geodetic, Aerial Photography, and Cartography Engineers]

UDC 778.534.83

[Abstract] Use of an afocal aberration compensator (L. Nefedov, OPTIKO- MEKHANICHESKAYA PROMYSHLENNOST No 6, 1961) in high-speed photographic cameras in addition to the 30-200 lenses, depending on the number of frames to be recorded, is considered as a way to compensate the higher-order chromatic as well as spherical aberrations produced by switching of these lenses. Such a compensator must not only correct the angular errors of a lens but also suppress the secondary spectrum due to differences between the refractive indexes for different wavelengths. Following a performance analysis of a "thin" compensator for one lens, based on applicable formulas of geometrical optics, a design analysis of such a compensator yields dimensional and optical data necessary for selection of the compensator material. Such a compensator with a high corrective power in C, D, and F light has been designed with plain glass rather than difficult to machine K1-crystal and with a minimum of optical surfaces in the intermediate objective. Figures 2; tables 1; references 8.

Mirror Compensator of Image Rotation

917F0163E Leningrad IZVESTIYA VYSSHIKH UCHEBNIKH ZAVEDENIY: PRIBOROSTROYENIYE in Russian No 12, Dec 90 pp 65-68

[Article by M.V. Dorofeyeva, State Institute of Applied Optics]

UDC 535.317.2

[Abstract] Considering that mirrors offer several advantages over prisms as compensators of image rotation in optical scanning systems, they are not aberrationless and less lossy but also easier to produce and at lower cost, their effectiveness when placed in the path of converging light rays between the objective and the plane of images is evaluated and compared with that of a prism compensator on the basis of their respective geometrical configurations. Two factors are taken into account, that a prism cannot transmit a cone of converging rays with an angle wider than the critical angle $\omega_{cr} = \tan^{-1}(n/2k)$ (n - refractive index of prism material, k - ratio of the length of path of light rays in the prism to the diameter of a cylindrical light beam) and that the refractive index of a mirror compensator is $n = 1$. A compensator consisting of three mirrors with a 120° angle between the first one and the third one has been designed for a cylindrical beam of light rays, with the same $k = 5.2$ ratio as in an Abbe prism. A design and performance analysis of this compensator, its field of view depending on the aperture stop of the objective and the critical angle for a conical light beam being 15°, confirms its suitability and indicates how it should be mounted. Figures 3; references 2.

**Design of Mirror Objectives With Planoidal
(Nearly Plane) Surfaces**

917F0163H Leningrad IZVESTIYA VYSSHIKH
UCHEBNYKH ZAVEDENIY: PRIBOROSTROYENIYE
in Russian No 12, Dec 90 pp 77-81

[Article by G.I. Tsukanova, Leningrad Institute of Precision Mechanics and Optics]

UDC 535.833

[Abstract] The design of three-mirror objectives with an almost aspherical and thus planoidal second or third mirror is analyzed, such a mirror having a large radius of curvature at the vertex and an infinitely large eccentricity squared. The analysis is based on the theory of third-order aberrations, these aberrations being usually compensated by surface deformation. Inasmuch as conventional three-mirror design methods are not applicable to planoidal mirrors, a new method is proposed which corrects not only spherical aberration but also coma and astigmatism. All three parallel mirrors, the

third mirror between the first and the second, are replaced with smooth surfaces and the following parameters are stipulated: distances $-d_1$ from first mirror to second mirror and d_2 from third mirror to second mirror, heights $h_1 > h_2 > h_3$ of null ray on the principal planes of all three mirrors, distance $-\delta$ from vertex of the second mirror to plane of the image, and angles α of null ray with the common optical axis. The null ray impinges on the first mirror parallel to the optical axis ($\alpha_1 = 0$ and leaves the third mirror at angle $\alpha_4 = h_1/F$ (F -second focal length), $\alpha_4 = -1$ in objectives with no intermediate image or with two intermediate images and $\alpha_4 = 1$ in objectives with one intermediate image after reflection by the first mirror or by two mirrors. The design procedure involves setting up and solving a system of equations which describes simultaneous full compensation of all three kinds of aberrations, in this case third-order aberrations of each kind. This system of equations yields expressions for the necessary deformations of mirrors. Numerical calculations have been made for both meridional and sagittal sections in an objective with a 1:4 relative aperture and 3° field of view angle.

On Problem of Evaluating Wind Energy Potential of Armenia

917F0183a Yerevan IZVESTIYA AKADEMII NAUK
ARMYANSKOY SSR: SERIYA TEKHNIЧЕСКИХ
NAUK in Russian No 4, 1990 pp 177-181

[Article by A. A. Mardzhanyan, G. S. Petrosyan, and K. V. Khachatryan. First paragraph is authors' abstract of article]

UDC 621.311.24:621.548

[Text] The specific energy characteristics of wind flow can be determined on the basis of Weibull distribution for regions promising from the viewpoint of developing wind energy. The parameters of the distribution can easily be calculated on the basis of statistical data on wind speeds using simple relations. A total of 1.5-2 billion kW x hr of electric power per year can be generated if 1,500-2,000 modern wind generating plants are installed in promising regions of Armenia.

Making the requirements more rigid on the ecological cleanliness of electric power generation and also the absence of local extractable types of fuel resources determined the timeliness of developing alternative energy in Armenia in general and of wind energy in particular. Accurate analysis of the wind energy potential and development of a wind cadaster are a necessary base for development of wind energy in the republic. A preliminary step of studies in this direction was developing a method of determining the energy characteristics of the wind flow at the wind vane level, developed at the Department of Electric Power Plants, Networks and Systems of YerPI [Yerevan Polytechnical Institute].

The basis of the method is approximation of the real probability density distribution of the wind speeds of a given locale using two-parameter Weibull distribution

$$f(u) = \frac{k}{c} \left(\frac{u}{c} \right)^{k-1} \exp \left[- \left(\frac{u}{c} \right)^k \right], \quad (1)$$

where u is wind speed at the height of the cadaster, m/s, $k > 0$ and $c > 1$ are Weibull distribution parameters.

A detailed description of calculating the values of parameters k and c on the basis of available statistical data on wind speeds for a given locale was presented in [1]. Let us dwell here on the problem of determining some specific energy characteristics of wind flow, which are of primary interest for solution of applied wind energy problems.

One can show [2, 3] that the kinetic energy of the wind flow is proportional to the value u^3 , multiplied by the probability that wind with given velocity will occur. Accordingly, to determine the value of wind speed with maximum energy, using expression (1), after simple transformations, we find

$$u_{me} = c \left(\frac{k+2}{k} \right)^{1/k} \quad (2)$$

The value of u_{me} permits one to determine the maximum energy included per unit surface of wind flow in a given locale through the year [4]

$$W_{bm} = \frac{1}{2} \rho u_{me}^3 f(u_{me}) 8760, \quad (3)$$

where $f(u_{me})$ is the probability of wind velocity with maximum energy, determined according to (1), and ρ is the density of air.

However, not all the energy determined by expression (3) can be used to generate electric power. In the ideal case, it is possible to use only 59.3 percent of the value of W_{bm} (the Betz limit [4]). Accordingly, the maximum electric power generated during the year with unit flow surface of an ideal wind turbine is determined according to

$$W_{em} = C_{pm} W_{bm}, \quad C_{pm} = 0.593. \quad (4)$$

The value of C_p , called the wind utilization factor, is less for real wind energy plants than the maximum value of C_{pm} , and is equal to (0.3-0.47) as a function of the type of wind turbine [3, 4].

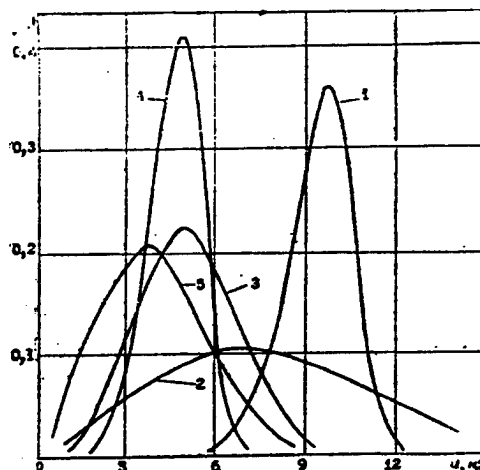


Figure. Probability Density Distribution Curves of Wind Speed According to Weibull for Different Regions

Key: 1. Sisian Pass; 2. Pushkin Pass; 3. Yeratumber; 4. Savan-ozernaya; 5. Aragats.

Based on available statistical information on the mean monthly values of wind speeds over a five-year period, Weibull distribution curves (figure) were plotted for five promising areas of the Armenian SSR, and the specific energy characteristics of wind flow were calculated

(table). As follows from the figure, the greatest shift of the maximum probabilities toward high wind speeds (> 5 m/s) are observed for the Sisian Pass. The distribution curve for the Pushkin Pass is distinguished by a more sloping nature compared to the others and has the

second shift of maximum probabilities toward the region of high velocities. The distribution curve for the Sevan-ozernaya region has a sharp peak for wind speeds of 4-5 m/s. It follows from the table that the region of the Sisian Pass has the greatest wind energy potential.

Table. Specific Energy Characteristics of Wind Flow

| Observation point | c, m/s | u_{me} , m/s | $f(u_{me})$ | W_{bm} , kW x hr/m ² | W_{am} , kW x hr/m ² |
|-------------------|-----------|----------------|-------------|-----------------------------------|-----------------------------------|
| Sisian Pass | 9.38/8.03 | 10.04/8.13 | 0.395/0.543 | 2,059/1,646 | 1,222/976 |
| Pushkin Pass | 7.79/6.47 | 11.75/8.73 | 0.054/0.101 | 497/382 | 295/225 |
| Yeratumber | 5.05/5.05 | 6.43/5.80 | 0.167/0.315 | 255/348 | 151/207 |
| Sevan-ozernaya | 4.73/4.18 | 5.35/4.53 | 0.379/0.651 | 329/343 | 195/604 |
| Argats | 4.11/4.03 | 5.95/5.46 | 0.120/0.160 | 143/148 | 85/88 |

1. Calculations were made for normal atmospheric conditions.

2. Data for 1981 are given in the numerator, while mean data for 5 years are given in the denominator

The reliability of calculations of the specific energy characteristics as a whole is determined by the accuracy of the initial meteorological information. The meteorological stations supplying this information in the republic are located to assemble averaged indicators—they are frequently on the territory of populated points or near them, and are shaded by structures, local features of relief and so on. Moreover, the complex mountainous relief of Armenia is an extremely significant flow-forming factor, and a sharp deformation of the surface layer of wind occurs due to its influence. Air masses are held and deflected by mountain ridges, and the stream is constricted and as a result the flow is accelerated in the passes and troughs of the ridges. The wind speed can increase 2-2.5-fold at slight distance of several hundred meters, due to the characteristics of the relief. This local acceleration of the flow is very significant for generation of electric power, since the capacity of the flow increases in proportion to the cube of wind speed. Thus, regions with an abundant wind potential fall out of the visual field of the existing network of meteorological stations and a synchronous measuring system that permits one to determine the three-dimensional pattern of wind flow in the troughs of ridges and in passes must be developed for full evaluation of it. Moreover, the methods of taking into account micrometeorological features of the studied regions and of variation of wind speed as a function of altitude must be worked out.

Having the specific energy characteristics of the wind flow of a given region, it is easy to calculate the annual generation of electric power, produced by using some of the existing industrial wind energy plants. Thus, let us consider a wind energy plant of the Nibe type (Denmark) with wind utilization factor of 0.42 and with air-swept surface of 1,257 m². If a given wind energy plant is installed in the region of the Sisian Pass, the maximum annual generation of electric power will comprise 1,659 MW x hr. Accordingly, if 600 of these wind energy plants are installed in this and other promising regions, annual generation of 1 billion kW x hr of electric power is possible. And if 1,500-2,000 modern wind energy plants

of medium capacities are located in promising regions of Armenia, 1.5-2 billion kW x hr of electric power annually can be generated. This number of installed wind energy plants is not unrealistic if a state program is adopted for development of wind energy. Thus, 1,500 wind energy plants were installed in Denmark in 1986, and approximately 200 new ones are turned over annually for operation, while more than 15,000 wind energy plants of medium capacities with total installed capacity of more than 600 MW were installed in the United States (California) for the same year.

Bibliography

1. Mardzhanyan, A. A., Petrosyan, G. S. "Evaluation of Armenia's Wind Energy Potential," "Energetika i elektrifikatsiya. Seriya Sooruzheniye gidroelektrostantsiy: Ekspres-informatsiya" [Energy and Electrification. Series Construction of Hydroelectric Power Plants: Express Information], Issue 12, 1988.
2. Lyatkher, V. M. "Vetrovyye elektrostantsii bolshoy moshchnosti" [High-Capacity Wind Electric Plants], Informenergo, 1987.
3. Renzo, D. de. "Vetroenergetika" [Wind Energy], Moscow, Izdatelstvo "Mir", 1982.
4. Johnson, G. L. Wind Energy Systems, New York, Prentice-Hall, 1985.

The UkSSR Coal Industry in 1990

917F0206A Kiev UGOL UKRAINY in Russian No 4, 1991 pp 55-62

[Unattributed article under the "Chronicles" rubric: "The UkSSR Coal Industry in 1990"]

[Text] In the past few years the republic's coal industry has experienced a reduction in its level of coal recovery and efficiency as a result of the aging of mine resources, an increase in the depth at which seams are developed, an increase in the complexity of geologic and mining

conditions, and unsatisfactory material and technical support of its mines. Various organizational flaws, a reduction in labor and industrial discipline, and a worsening of the social economic conditions of miners' labor and daily living conditions have all had a negative effect on work in the sector. The system of measures stipulated by government decree No. 608 has not been fully implemented. This has created tension in the republic's coal

basins. All of these shortcomings reduced the sector's operating efficiency in 1990.

Compared with 1989, the recovery of all coals in 1990 has been reduced by 4.47 million tons, amounting to 175.7 million tons. This in turn is only 93.8% of the planned figure (Table 1). Except for the Aleksandriyugol, no association has fulfilled its coal recovery plan. Most are noticeably below their yearly coal recovery volume.

Table 1.

| Production Association | Recovery of All Coals | | | | Recovery of Coals for Coking | | | |
|------------------------|----------------------------|---------------------------|--------------------|---------------------------|------------------------------|---------------------------|--------------------|---------------------------|
| | Planned, thousands of tons | Actual, thousands of tons | Percentage of Plan | Percentage of 1989 Amount | Planned, thousands of tons | Actual, thousands of tons | Percentage of Plan | Percentage of 1989 Amount |
| Donetsk Oblast | 85,148 | 80,451 | 99.5 | 91.7 | 49,899 | 47,754 | 95.7 | 91.0 |
| Donetskugol | 19,160 | 18,728 | 97.7 | 92.7 | 14,572 | 14,301 | 98.1 | 90.7 |
| Makeyevugol | 11,930 | 11,207 | 93.9 | 91.8 | 11,365 | 10,733 | 94.4 | 91.7 |
| Krasnoarmeyskugol | 8,690 | 8,462 | 97.4 | 89.8 | 8,300 | 8,079 | 97.3 | 90.3 |
| Selidovugol | 5,315 | 5,184 | 97.5 | 93.2 | - | - | - | - |
| Dobropolyeugol | 6,955 | 6,817 | 98.0 | 97.1 | 5,440 | 5,328 | 97.9 | 99.2 |
| Artemugol | 5,963 | 5,390 | 90.4 | 85.2 | 5,412 | 4,893 | 90.4 | 84.7 |
| Dzerzhinskugol | 2,840 | 2,591 | 91.2 | 88.2 | 2,840 | 2,591 | 91.2 | 88.2 |
| Ordzhonikidzeugol | 4,555 | 4,086 | 89.7 | 85.1 | 1,570 | 1,433 | 91.2 | 91.7 |
| Shakhterskugol | 4,870 | 4,560 | 93.6 | 97.1 | - | - | - | - |
| Oktyabrugol | 6,630 | 5,987 | 90.3 | 93.2 | 400 | 396 | 99.1 | 97.8 |
| Torezantratsit | 8,240 | 7,439 | 90.3 | 91.7 | - | - | - | - |
| Lugansk Oblast | 55,975 | 51,619 | 92.2 | 93.1 | 12,450 | 11,813 | 94.9 | 99.2 |
| Luganskugol | 8,400 | 8,004 | 95.3 | 93.7 | 400 | 369 | 92.2 | 104.2 |
| Stakhanovugol | 6,305 | 6,017 | 95.4 | 98.7 | 3,005 | 2,870 | 95.5 | 98.5 |
| Pervomayskugol | 3,850 | 3,242 | 84.2 | 92.4 | 1,595 | 1,307 | 81.9 | 94.2 |
| Lisichanskugol | 3,280 | 3,162 | 96.4 | 102.9 | - | - | - | - |
| Krasnodonugol | 7,600 | 7,362 | 96.9 | 100.2 | 7,450 | 7,267 | 97.5 | 100.2 |
| Donbassantratsit | 7,000 | 6,080 | 86.9 | 85.4 | - | - | - | - |
| Antratsit | 4,140 | 3,432 | 82.9 | 81.1 | - | - | - | - |
| Rovenkiantratsit | 7,200 | 6,773 | 94.1 | 91.8 | - | - | - | - |
| Sverdlovantratsit | 8,200 | 7,541 | 92.0 | 92.2 | - | - | - | - |
| Pavlogradugol | 13,515 | 12,986 | 96.1 | 90.8 | 3,093 | 3,102 | 100.3 | 136.3 |
| Ukrzapidugol | 11,830 | 10,524 | 89.0 | 82.3 | 5,720 | 5,118 | 89.5 | 85.5 |
| Aleksandriyugol | 9,230 | 9,231 | 100.0 | 85.6 | - | - | - | - |
| Throughout UkSSR | 175,698 | 164,810 | 93.8 | 91.5 | 71,162 | 67,787 | 95.3 | 93.3 |

The underground method was used to recover 158.3 million tons of coal (93.3% of the plan and 91.3% of the 1989 level), and the open-pit method was used to recover 6.5 million tons of coal (106.5 and 97.1%, respectively). The hydraulic method was used to recover 2.8 million tons (105 and 98%). The average daily recovery of coal in the republic equaled 480,000 tons as opposed to the figure of 518,000 tons stipulated in the plan. Recovery from 1 square meter of the web area of a seam amounted

to 1.78 tons, which is 7.5% above the indicator stipulated in the plan and 0.6% of the 1981 indicator.

Coals for coking were recovered in the amount of 67.8 million tons or 95.3% of the amount stipulated in the plan and 93.3% of the 1989 level. The only association to meet the plan for recovery of coal for coking was the Pavlogradugol Association, which is located in an area

where recovery of such coals has increased in recent years. It has, however, dropped noticeably in the central region of the Donbass at the Pervomayskugol and Ukrzapidugol associations.

In 1990, 206.5 million tons of coal was delivered to consumers. This was 2.2 million tons short of the plan. Many mines and associations did not meet their contractual obligations. The ash content of the coal recovered amounted to 29.6% with a standard of 29.6%. The ash content of coal delivered was 17.8% versus a norm of 18.4% and was 0.6% lower than in 1989. Balances at warehouses holding all coals equaled 4,720,000 tons as opposed to the standard-specified amount of 4,240,000 tons. The balances of coals for coking amounted to 846,000 tons versus the 1,090,000 tons called for in the standard.

Prepared coal reserves in sections amounted to 1,947,000 tons, whereas the plan called for 2,115,000 tons; 785,000 tons was prepared for removal, whereas the plan called for preparing 900,000 tons for removal. The amount of stripping operations was lower than in 1989.

Table 2 gives performance indicators both for all development openings (by the fiscal and contractual methods) and for stripping and development operations. The figure for total developments fell 3% short of the plan and 3.7% short of the 1989 level. The corresponding figures for stripping and development operations were 7.1 and 9.2%, respectively.

Table 2.

| Production Association | Development Openings (by the fiscal and contractual methods) | | | | | |
|------------------------|--|--------------------|---------------------------|-------------------------------------|--------------------|---------------------------|
| | Total | | | Including Stripping and Development | | |
| | Actual, km | Percentage of Plan | Percentage of 1989 Amount | Actual, km | Percentage of Plan | Percentage of 1989 Amount |
| Donetsk Oblast | 1,210.7 | 98.3 | 90.2 | 897.1 | 93.7 | 90.9 |
| Donetskugol | 218.2 | 90.2 | 85.8 | 183.1 | 89.9 | 89.4 |
| Makeyevugol | 165.1 | 98.3 | 88.2 | 129.8 | 95.5 | 91.6 |
| Krasnoarmeyskugol | 78.8 | 96.8 | 93.0 | 75.4 | 98.9 | 95.4 |
| Selidovugol | 68.3 | 88.0 | 84.8 | 60.9 | 87.6 | 85.5 |
| Dobropolyeugol | 109.8 | 88.9 | 89.6 | 73.9 | 88.7 | 88.7 |
| Artemugol | 135.8 | 101.1 | 92.1 | 96.1 | 98.7 | 93.8 |
| Dzerzhinskugol | 77.4 | 105.6 | 90.9 | 45.4 | 92.1 | 90.8 |
| Ordzhonikidzeugol | 104.9 | 117.3 | 95.5 | 67.3 | 101.9 | 90.5 |
| Shakhterskugol | 72.2 | 110.7 | 100.4 | 46.0 | 101.9 | 95.2 |
| Oktyabrugol | 68.8 | 93.4 | 91.2 | 51.6 | 86.9 | 90.6 |
| Torezanratsit | 111.6 | 108.4 | 90.2 | 67.7 | 94.3 | 90.6 |
| Lugansk Oblast | 730.5 | 94.8 | 90.8 | 532.5 | 90.0 | 90.8 |
| Luganskugol | 121.4 | 98.3 | 94.6 | 93.2 | 94.8 | 94.0 |
| Stakhanovugol | 137.0 | 105.6 | 97.7 | 94.9 | 98.6 | 98.3 |
| Pervomayskugol | 61.1 | 97.9 | 89.2 | 48.1 | 89.1 | 94.2 |
| Lisichanskugol | 40.4 | 77.5 | 82.1 | 36.2 | 77.3 | 80.0 |
| Krasnodonugol | 90.8 | 93.7 | 90.4 | 73.0 | 89.6 | 90.5 |
| Donbassanratsit | 81.6 | 89.3 | 86.9 | 49.8 | 86.8 | 90.3 |
| Anratsit | 37.8 | 79.8 | 79.5 | 29.6 | 78.3 | 82.4 |
| Rovenkianratsit | 71.1 | 91.6 | 86.9 | 43.2 | 85.0 | 82.8 |
| Sverdlovanratsit | 89.3 | 99.3 | 94.9 | 64.5 | 94.1 | 91.7 |
| Pavlogradugol | 152.3 | 99.5 | 95.5 | 142.8 | 99.3 | 94.7 |
| Ukrzapadugol | 112.8 | 94.4 | 85.7 | 97.6 | 91.5 | 86.2 |
| Aleksandriyugol | 25.7 | 101.3 | 80.6 | 23.8 | 100.3 | 81.2 |
| Throughout UkSSR | 2,232.0 | 97.0 | 96.3 | 1,693.7 | 92.9 | 90.8 |

As is evident from Table 2, most associations failed to meet the plan for sinking shafts. This confirms the fact that the

situation regarding preparation of a clean front is unsatisfactory at many mines. The figures for the percentage of the

plan for opening developments met at the Selidovugol, Dobropolyeugol, Oktyabrugol, and Lisichanskugol associations were especially low. Only three associations (the

Ordzhonikidzeugol, Shakhterskugol, and Aleksandriyugol) met their plan indicators for both development openings and stripping and development workings.

Table 3.

| Production Association | Average Active Number of Cleared Faces | Average Monthly of Face Advance, m | Average Active Line of Cleared Face, km | Average Daily Load on an Active Cleared Face, t |
|------------------------|--|------------------------------------|---|---|
| Donetsk Oblast | 894.4 | 28.6 | 130.4 | 263 |
| Donetskugol | 191.5 | 26.4 | 32.2 | 295 |
| Makeyevugol | 121.9 | 25.9 | 19.5 | 265 |
| Krasnoarmeyskugol | 33.7 | 50.2 | 62.6 | 766 |
| Selidovugol | 33.0 | 46.1 | 49.7 | 464 |
| Dobropolyeugol | 33.2 | 66.8 | 46.1 | 676 |
| Artemugol | 132.9 | 23.1 | 14.3 | 120 |
| Dzerzhinskugol | 68.5 | 19.5 | 7.9 | 107 |
| Ordzhonikidzeugol | 105.6 | 22.8 | 11.3 | 107 |
| Shakhterskugol | 41.8 | 25.3 | 8.2 | 285 |
| Oktyabrugol | 54.0 | 28.7 | 10.1 | 336 |
| Torezantratsit | 78.3 | 25.8 | 12.0 | 271 |
| Lugansk Oblast | 459.1 | 28.7 | 77.6 | 338 |
| Luganskugol | 66.4 | 33.6 | 10.9 | 336 |
| Stakhanovugol | 95.7 | 20.3 | 15.2 | 181 |
| Pervomayskugol | 37.4 | 21.1 | 6.8 | 272 |
| Lisichanskugol | 22.4 | 33.5 | 3.9 | 473 |
| Krasnodonugol | 56.7 | 33.4 | 9.0 | 386 |
| Donbassantratsit | 67.6 | 24.0 | 11.6 | 295 |
| Antratsit | 31.7 | 21.3 | 5.7 | 342 |
| Rovenkiantratsit | 40.4 | 35.9 | 7.6 | 495 |
| Sverdlovantratsit | 40.8 | 48.3 | 6.7 | 572 |
| Pavlogradugol | 69.5 | 62.9 | 11.8 | 568 |
| Ukrzapadugol | 74.9 | 41.7 | 11.1 | 463 |
| Aleksandriyugol | 16.5 | 41.7 | 1.4 | 580 |
| Throughout UkSSR | 1,409.8 | 30.9 | 226.3 | 311 |

Table 3 presents technical mining indicators with respect to all cleared faces and to working faces equipped with mechanized systems (abbreviated KMZ). Compared with 1989, the average active number of cleared faces in 1990 decreased by 53. Their average active line was reduced by 5.3 km, and the average monthly face advance was reduced by 2.4 m. The average daily recovery from an active cleared face was less than 8 tons. The average active number of working faces equipped with mechanized systems remained practically at the 1989 level; their average active line increased by 1.9 km. The average daily load was 1.6% above the amount specified in the plan but 3.4% less than the 1989 level.

In 1990 the relative share of workings made with mechanized loading of coal and ore amounted to the following (the data presented in parentheses include cutter-loaders): throughout the UkSSR, 81.3% (33%); through the Donetsk Oblast, 83.9% (32.1%); for the Donetskugol,

85.8% (37.4%); for the Makeyevugol, 76.8% (30.2%); for the Krasnoarmeyskugol, 98.5% (79%); for the Selidovugol, 80.6% (43.6%); for the Dobropolyeugol, 96.7% (74%); for the Artemugol, 100% (0.9%); for the Dzerzhinskugol, 99.6% (0.6%); for the Ordzhonikidzeugol, 92.1% (0%); for the Shakhterskugol, 59.0% (23.4%); for the Oktyabrugol, 64.1% (16.6%); for the Torezantratsit, 67.4% (6.8%); throughout the Lugansk Oblast, 72.2% (12%); for the Luganskugol, 80.4% (20.1%); for the Stakhanovugol, 76.5% (3.4%); for the Pervomayskugol, 66.0% (10.3%); for the Lisichanskugol, 86.1% (37.3%); for the Krasnodonugol, 83.4% (29.2%); for the Donbassantratsit, 81.8% (11.6%); for the Antratsit, 59.0% (1.9%); for the Rovenkiantratsit 48.1% (6.3%); for the Sverdlovantratsit, 65.0% (1.2%); for the Pavlogradugol, 98.0% (96.8%); for the Ukrzapadugol, 86.5% (68.9%); and for the Aleksandriyugol, 74.3% (74.3%).

Table 4 presents key operating indicators for the year for the republic's coal enrichment facilities. A total of 132.02

million tons of coal was processed, and 81.65 million tons of concentrate was obtained. The yield of coals belonging to the coarse and medium classes amounted to 19.66 million tons, including 12.81 tons of anthracites. About 4 million tons of coal briquettes were produced. As is evident from

Table 4, however, the figures stipulated in the plan were not reached. Furthermore, a decrease in all indicators when compared with the data for 1989 was noted. This was largely due to a decrease in the volumes of coal that was recovered and sent for enrichment.

Table 4.

| Indicator | Enrichment of coals | | | |
|---|----------------------------|---------------------------|--------------------|---------------------------|
| | Planned, thousands of tons | Actual, thousands of tons | Percentage of Plan | Percentage of 1989 Amount |
| Coal processing at enrichment plants | 142,076 | 132,023 | 92.9 | 94.1 |
| Including for coking | 56,772 | 54,340 | 95.7 | 97.4 |
| Output of concentrate | 86,255 | 84,646 | 94.7 | 94.6 |
| Including for coking | 35,570 | 34,544 | 97.1 | 97.7 |
| Output of Coarse- and Medium-Class Coals | 21,162 | 19,661 | 92.9 | 91.1 |
| Including anthracites | 14,001 | 12,812 | 91.5 | 91.6 |
| Coal processing at mechanized spoil-picking installations | 11,306 | 11,061 | 97.8 | 94.4 |
| Production of coal briquettes | 4,020 | 3,991 | 99.3 | 95.7 |

Enterprises' production of consumer products at optimum prices was 4.3% below the amount stipulated in the plan. It was 4.6% lower in calculated prices. The production cost of 1 ton coal in January-November 1990 amounted to 34.87 rubles versus the 32.47 rubles stipulated in the plan, and it was 5.94 rubles higher than the amount for the same period of 1989. The average monthly number of industrial and production personnel in the republic's coal industry was 15,600 less than the number specified in the plan and 5,500 less than the 1989 figure. The output of consumer product per worker was as follows: throughout the entire UkSSR, 8,551 rubles versus the the 8,758 rubles stipulated in the plan; throughout the Donetsk Oblast, 7,445 rubles (7,600 rubles in the plan); and throughout the Lugansk Oblast, 9,219 rubles (9,506 rubles in the plan).

In 1990 production facilities to recover coal in the amount of 4,870,000 tons per year were introduced into the coal

industry of the UkSSR. The first phase of the Krasnoarmeyskaya-Zapadnaya mine of the Krasnoarmeyskugol Production Association, which has a capacity of 1,500,000 t/y, was put into operation. Also put into operation were the second phases of the following mines: the Shakhterskaya-Glubokaya (Shakhterskugol), which has a capacity of 1,200,000 t/y; the Komsomolets Donbassa (Oktyabrugol), which has a capacity of 550,000 t/y; and the Luganskaya No. 1 (Luganskugol), which has a capacity of 500,000 t/y. As a result of reconstruction, the capacity of the mine Komso-molskaya (Antratsit) increased by 400,000 tons, and that of the mine Krasnyy partizan (Sverdlovantratsit) increased by 100,000 tons. The Konstantinovskiy section of the association Aleksandriyugol (capacity, 500,000 tons of coal per year) was also put into operation.

COPYRIGHT: Ukrainskoye respublikanskoye uprov-leniye VNTO Gornoye, 1991.

Dynamics of Asymmetric Interaction Involving Body of Revolution and Rigid Barrier*917F0196A Kiev PRIKLADNAYA MEKHANIKA in Russian No 11, Nov 90 pp 31-35*

[Article by I.Ye. Khorev and N.T. Yugov, Scientific Research Institute of Applied Mathematics and Mechanics, Tomsk]

UDC 539.3

[Abstract] Asymmetric interaction of an undeformable barrier and steel cylinders striking it obliquely is considered, of concern being the dynamics of this interaction and specifically the energy transfer during impact. The interaction is analyzed on the basis of numerical calculations made by the method of finite elements in accordance with the elastoplastic model of continuous media. Such calculations were made for three cylinders with the same initial diameter ($D = 0.0125$ m) but different length-to-diameter ratios ($L/D = 1, 2, 3$). Each cylinder was made to strike the barrier obliquely at various angles ($15^\circ, 30^\circ, 45^\circ, 60^\circ, 75^\circ$) and with various velocities ($V = 100$ m/s, 300 m/s, 500 m/s) at each angle. The analysis covers a transient period of 200 μ s. It reveals how the deformation of a cylinder as well as its pressure force and loss of kinetic energy as functions of time during that period depend not only on its initial relative length and its velocity but also on the angle of impact. The results of this analysis give a better insight into the mechanism of ricochet. Figures 4; tables 2; references 10.

Experimental Study of Dynamic Deformation of Hollow Elastic Cylindrical Shells Immersed in Water and Vacuumized*917F0196B Kiev PRIKLADNAYA MEKHANIKA in Russian No 11, Nov 90 pp 49-55*

[Article by I.I. Anikyeu, M.I. Mikhaylova, and Ye.A. Sushchenko, Institute of Mechanics, UkSSR Academy of Sciences, Kiev]

UDC 539.3

[Abstract] An experimental study of thin hollow circular elastic cylindrical shells under static pressure produced by immersion in water and vacuumization was made, of interest being their dynamic deformation by a weak and short subcritical pressure pulse under these conditions. The experiment was performed with 330 mm long and 120 mm in diameter, 0.4 mm thick shells of D16T duralumin turned on a lathe and 0.8 mm thick shells of glass-plastic (seven layers of E-3-10 glass cloth tape with EF 32-301-16 binder: ED-16 epoxy resin + bakelite varnish + acetone). Their walls were sealed by coating of shellac on the outside surface and their both ends were tightly closed by plugs, a pipe connected to a suction pump passing through one of them. After having been tested in air for residual strains, each shell was immersed to certain depth within the 1.1-1.5 m range in water

filling a 3 m high cylindrical tank 3.2 m in diameter and air was from its cavity. A pressure wave in water was then generated by explosion of a 15 mm long copper wire 0.1 mm in diameter, through which a 48 μ F - 2.5 kV battery of IKM-25-12-U4 noninductive capacitors had been discharged. The amplitude of the acoustic wave was about 0.3 MPa, varying from test to test but only within $\pm 3.5\%$, and its steep front at a distance of 0.5 mm from the wire was followed by an exponential pressure fall with a time constant of about 50 μ s. For measurements were used KF5P1-1-200A-12 strain gages with a 1 mm base or KF5P4-3-100V-12 strain gages with a 3 mm base in a TsTM-5 digital tensometer bridge. The error of pressure settings did not exceed 5 % and the error of strain readings was accurate within about 10 %. Pressure and strains were also recorded on an S8-13 oscillograph over a transient period of 1.2 ms. All shells were found to behave as imperfect ones, hydrostatic pressure thus produced in them flexural as well as membrane strains. No strain of any shell exceeded 0.003 within the elastic range. The results indicate that a weak and short pressure pulse causes the dynamic membrane strains of such shells under a static load to alternate, their amplitude being larger and their duration being longer in the first compression half-cycle than in the following ones, and the magnitude of dynamic flexural strains during the tension-compression cycle depends largely on the total static pressure load. Figures 4; references 10.

Nonlinear Deformation of Cylindrical Shell by Local Thermal Shock*917F0196C Kiev PRIKLADNAYA MEKHANIKA in Russian No 11, Nov 90 pp 55-60*

[Article by N.I. Obodan and N.B. Makarenko, Dnepropetrovsk University]

UDC 539.3

[Abstract] Nonaxisymmetric deformation of thin-walled cylindrical shells and panels by fast local heating under uniform external pressure is analyzed on the basis a geometrically and physically nonlinear model which combines the theory of flat shells with the incremental deformation theory of plasticity. The total strain is accordingly expressed as the algebraic sum of its elastic, thermal, and plastic components. The two equations, of motion and of compatibility of strains, are solved for homogeneous initial conditions and boundary conditions of circumferential periodicity (closed shells) or boundary conditions at the edges (cylindrical panels). The transient temperature field in a shell is found by solving Fourier's parabolic second-order partial differential equation of heat conduction for zero initial conditions and boundary conditions of convective heat transfer to the ambient medium, from a bare lateral surface and insulated bases. Integration of this equation yields two components of the temperature field: temperature of the median surface and temperature difference

across the wall thickness. A system of ordinary differential equations is then constructed for deflections and both components of its temperature field. This system of equations being can be solved numerically by the Runge-Kutta method, after reduction to the Cauchy problem and determination of the initial displacement vector for each time step by Newton's method. The problem was solved for cylindrical steel shells 0.1 mm thick and 2.0 cm long with a 4.3 cm radius first under zero static pressure, then successively under static pressures equal to 60 % and 85 % critical, while being heated by a locally incident thermal flux at characteristic rates of 5×10^n °C/s ($n = 0, 2, 4, 6, 8$). The results indicate that plastic deformation begins sooner as the heating rate is increased, the region of plastic deformation expanding slowly when the heating rate is low (quasi-static deformation) and spreading instantaneously over the entire thickness of the shell or panel wall when the heating rate is high (dynamic deformation). In the latter case the size of the heat spot and thus the degree of thermal flux localization is not an influencing factor. Intermediate heating rates thus cover the range associated with strong interplay of comparable static and dynamic deformation effects. Figures 5; references 12.

Transient Processes in Electrically Excited Multilayer Piezoceramic Stack

917F0196D Kiev PRIKLADNAYA MEKHANIK
in Russian No 11, Nov 90 pp 61-66

[Article by A.E. Babayev and V.G. Savin, Institute of Mechanics, UkSSR Academy of Sciences, Kiev]

UDC 539.6.013.42

[Abstract] Transient processes in a piezoelectric stack of N plane layers following its excitation by an electric pulse signal are analyzed on the basis of the linear theory of electroelasticity. All layers have the same thickness h and identical mechanical properties. The lower surface of the bottom layer adheres rigidly to a base ($z = 0$) and the upper surface of the top layer ($z = Nh$) is load-free, but the electric pulse impinges on that surface of the top layer ($k = N$) and then continues passing through successive interlayer boundaries (layers $k = N-1, \dots, 2, 1$). The corresponding three systems of k equations ($k = 1, 2, \dots, N$), two equations involving normal displacements and electric potentials and one equation involving normal stresses and electric potentials for each layer, are solved for boundary conditions of unbroken contact between layers, zero normal displacement of lower surface of bottom layer ($k = 1$), compatible normal displacements of all interlayer boundaries and compatible normal stresses at all interlayer boundaries ($k = 1, 2, \dots, N-1$), zero normal stress at the upper surface of top layer ($k = N$), electric potentials $\Psi^{(k)} \setminus v_{z-k-1} = (-1)^{k-1} Q(t)H(t)$ and $\Psi^{(k)}|_{z-k} = (-1)^k Q(t)H(t)$ ($k = 1, 2, \dots, N$). Here function $Q(t)$ characterizes the waveform of the incident electric signal and $H(t)$ is Heaviside's unit function. Following

elimination of the electric potential from the two equations where it appears with displacements, the remaining two systems of equations are solved by the Laplace transformation method. The results of a numerical analysis for a piezoelectric transducer made of TsTBS-3 (B, Sr zirconate-titanate) indicate how the variation of its stress and strains depends on the number of layers and the signal waveform. Figures 5; references 5.

Nonaxisymmetric Stressed and Strained State of Anisotropic Multilayer Shells of Revolution

917F0196E Kiev PRIKLADNAYA MEKHANIK
in Russian No 11, Nov 90 pp 66-70

[Article by G.M. Kulikov, Tambov Institute of Chemical Apparatus Design]

UDC 539.3

[Abstract] A stress and strain analysis is performed for nonorthotropic shells of revolution with uniform thickness consisting of N anisotropic layers, each layer having a different uniform thickness. The reference surface is placed in a system of curvilinear orthogonal coordinates α_1 and α_2 , its curvature and the Lamé parameter A_1 then being functions of only one variable α_1 . The resolvent system of ten partial differential equations is supplemented with four differential and four algebraic relations for the relevant shell constants and variables, also with a fourth-order matrix equation for forces and moments. The system is then solved for zero boundary conditions identical to the classical boundary conditions in the Kirchhoff-Love theory of shells. The solution is expressed in the form of two vectors $X(\alpha_1$ and $\alpha_2)$, both as well as the load q assumed to be expandable into complete Fourier series on the $[-\pi, \pi]$ interval. That system of partial differential equations thus reduces to a one of ordinary differential ones which can be integrated by the method of discrete orthogonalization, those four differential relations being reduced to algebraic ones. The algorithm of calculating the deflection in this way has been programmed in the PL/1(0) version of the high-level PL/1 language in the form of the main ANST3 procedure, for execution on a Standard System 1060 computer. The procedure was tested first on a homogeneous transversely isotropic cylindrical shell with rigid constraints at both ends while under a normal load $q = q_0 \cos \alpha_2$, then on a cylindrical shell consisting of two orthogonally wound boron-plastic layers with similar constraints at both ends while under a similar load. Figures 2; tables 1; references 7.

Dispersion Equations for Electroelastic Shear Waves in Multilayer Media With Periodic Structure

917F0196F Kiev PRIKLADNAYA MEKHANIK
in Russian No 11, Nov 90 pp 84-93

[Article by L.P. Zinchuk, A.N. Podlipenets, and N.A. Shulga, Institute of Mechanics, UkSSR Academy of Sciences, Kiev]

UDC 539.3:534.1

[Abstract] Dispersion equations for surface acoustoelectric shear waves in multilayer media with periodic structures are derived, media considered here being those in the crystallographic 6mm class such as a wurtzite crystal or polarized piezoceramics. Propagation of such a wave through such a medium in an xy plane is described by a system of six partial differential equations for the stress tensor components σ_{xx} and σ_{zy} , the displacement w , the electric-displacement vector components D_x and D_y , and the electrostatic potential ϕ . The solution to it is sought in the form unordered set: $D_y(x, y, t)$, $\sigma_{zy}(x, y, t)$, $\phi(x, y, t)$, $w(x, y, t)$ = unordered set: $q_1(y)$, $q_2(y)$, $p_1(y)$, $p_2(y)$ $e^{ikx - i\omega t}$ (t - time, ψ - radian frequency of wave, k - wave number). For this the system of equations is transformed into one of ordinary differential ones for vectors $q = \text{col}(q_1, q_2)$ and $p = \text{col}(p_1, p_2)$. The monodromy matrix $U(h)$ of this h -periodic Hamiltonian system has a characteristic equation $\det[U(h) - \kappa E] = 0$ which, according to the Lyapunov-Poincare recurrence theorem, is $\kappa^4 + a_1\kappa^3 + a_2\kappa^2 + a_1\kappa + 1 = 0$. The dispersion equations for surface shear waves in such a medium are constructed on this basis, for a medium occupying the upper half-space $y > 0$ with $\sigma_{zy}(x, 0, t)$ and $\phi(x, 0, t) = 0$ conditions at its boundary $y = 0$ with vacuum below. For a dispersion analysis of waves in media with specific structures, one can evaluate both the monodromy matrix $U(h)$ and its matrizant $U(y)$ in that system of ordinary differential equations or solve the Cauchy problem for that system numerically by the Runge-Kutta method. Such an analysis is demonstrated on three examples: 1) surface waves in a structure formed by alternating layers of TsTC-19 (Sr zirconate-titanate) piezoceramic and epoxy resin, 2) surface waves in a structure formed by alternating layers of crystalline CdS and ZnO, 3) normal waves in a structure formed by layers of crystalline CdS and ZnO. Figures 6; tables 1; references 23.

Use of Asymptotic Method for Analysis of Finite-Amplitude Vibrations of Flat Shells

917F0196G Kiev PRIKLADNAYA MEKHANIKA
in Russian No 11, Nov 90 pp 93-99

[Article by N.I. Zhinzher and V.Ye. Khromatov,
Moscow Institute of Energetics]

UDC 539.3:534.1

[Abstract] Nonlinear free vibrations of thin elastic and isotropic shells, rectangular in the plan view with sides a_1, a_2 and thickness h , are described by Andrianov's simplified integrodifferential equations (I.V. Andrianov, PRIKLADNAYA MATEMATIKA I MEKHANIK Vol 50 No 1, 1986) analogous to Berger's equations for plates but with the median surface referred to system of curvilinear coordinates x_1, x_2 coinciding with the principal curvature lines. This system of equations is solved by Bolotin's asymptotic method (V.V. Bolotin, "Random Vibrations of Elastic Systems", Izd. "Nauka" 1979; IZV. AKADEMII NAUK SSSR: MEKHANIKA I

MASHINOSTROYENIYE No 4, 1962) for small vibrations far from the edges of the shell and thus non-momentary ones. Insertion of the generating solution for the deflection function within this region into that system system of equations yields a resolvent equation which relates the frequency of nonlinear vibrations to their amplitudes and wave number through elliptic functions. Numerical calculations by this method reveal how the distribution of natural frequencies depends on the amplitude of vibrations, as demonstrated on a plate. Figures 5; references 8.

Forced Longitudinal Oscillations of Long Pipe Containing Liquid

917F0196H Kiev PRIKLADNAYA MEKHANIK
in Russian No 11, Nov 90 pp 114-118

[Article by V.S. Tikhonov, V.I. Komissarenko, and B.V. Yemets, Central Scientific Research Institute of Geological Exploration, Moscow]

UDC 534.11:622.648

[Abstract] Equations of motion are derived to describe longitudinal oscillations of a long pipe driven into the ocean bed for exploration, such a pipe containing a column of liquid above the mud which plugs it at the bottom. The equations are based on a linear relation between the change of pressure and the bulk train of the liquid column, assuming that the liquid is a linearly compressible one, and an analogous relation for the linearly elastic pipe in accordance with Hooke's law. To the two ordinary differential equations of statics for infinitesimally small pipe and liquid column segments are added two partial differential equations of dynamics for the longitudinal forces acting on them in accordance with Newton's second law, including not only the pressure force and gravity but also viscous friction against surrounding sea water. Transformation of these equations in four real variables (x - displacement of pipe, X - displacement of liquid column, ΔF - increment of pressure force on liquid, ΔT - increment of tension force on pipe) as functions of time into equations in corresponding four complex variables as functions of frequency reduces them to a linear boundary-value problem for a system of four ordinary differential equations which can be solved numerically by the ranging method. This has been done for a 6000 m long steel drill column with a 0.146 m inside diameter and a 0.168 m outside diameter, weighing 41.5 kg/m and containing water, assuming a $w(\omega) = \text{const}$ amplitude-frequency characteristic and a $\psi(\omega) = 0$ phase-frequency characteristic of platform heaving. Figures 1; references 4.

Propagation of Shear Waves Through Nonlinearly Elastic Body

917F0164OI Kiev PRIKLADNAYA MEKHANIK
in Russian No 1, Jan 91 pp 127-129

[Article by V.I. Yerofeyev and I.G. Raskin, Institute of Machine Science, USSR Academy of Sciences, Nizhne-gorodskiy branch]

UDC 539.3

[Abstract] Propagation of plane shear waves through an isotropic nonlinearly elastic body is described by a wave equation with a coefficient α in the $\alpha/p(\delta u/\delta x)^2 \delta^2 u/\delta x^2$ term (u - transverse displacement) which additively combines the effects of quadratic, cubic, and quartic elasticity nonlinearities. The solution to this equation is, in the linear approximation, represented as a series of harmonics whose frequencies ω_j and wave numbers k_j are related through the dispersion equation $\omega_j - c_\tau k_j$ ($c_\tau = (\mu/\rho)^{1/2}$ denoting the velocity of shear waves, ρ - density of material, μ - Lamé constant of second order). In the case of a strong cubic nonlinearity the effect of self-action dominates over generation of higher-order harmonics so that the latter may be ignored. The solution can in this case be sought in the form of a single harmonic with a complex amplitude which slowly varies in space and in time. It is found by averaging over "fast" variables. A random process in a body with cubic nonlinearity is considered, a Gaussian noise for specificity, and its time correlation function $B(\tau, x)$ is found in a form which facilitates solution of the following inverse problem: to calculate the coefficient of cubic nonlinearity from the change in spectral width of a noisy shear wave. Numerical calculations were made for a noisy shear wave with a frequency of about 5 MHz propagating through a specimen of cubically nonlinear D16T aluminum alloy with a strain $\delta u/\delta x \approx 0.0003$ and a $\Delta\omega_k/\Delta\omega_0 \approx 1.1$ or 10 % change in the width of its spectrum, the nonlinearity coefficient being $\alpha = 10^7$ N/mm². The authors thank A.I. Vesnitskiy for discussing the results. References 5.

Longitudinal Damped Vibrations of Plates

917F0164H Kiev PRIKLADNAYA MEKHANIKA
in Russian No 1, Jan 91 pp 124-127

[Article by A.S. Kosmodamianskiy, Donetsk University, and M.N. Gofman, Mariupol Institute of Metallurgy]

UDC 539.3

[Abstract] Longitudinal vibrations of a plate with arbitrary smooth outer and inner contours moving under a periodically fluctuating pressure while overcoming a resistance force proportional to its velocity are analyzed by Kosmodamianskiy's approximate method for steady-state vibrations of multiply-connected bodies (A.S. Kosmodamianskiy, VESTNIK UKSSR AKADEMII NAUK No 4, 1988). Inasmuch as damped vibrations are of concern here, the two components of the displacement vector $U(x, y, t)$, $V(x, y, t)$ in the system of two partial differential equations of motion relating gradients of stresses $\sigma_{x,y}$, τ_{xy} to components of vibration velocity $\alpha \delta U/\delta t$, $\alpha \delta V/\delta t$ and components of vibration acceleration $\rho \delta^2 U/\delta t^2$, $\rho \delta^2 V/\delta t^2$ are expressed in the form $A(x, y)e^{(i\omega - \alpha/2p)t}$ (ω - frequency of pressure fluctuations, α - damping coefficient). After insertion of Hooke's law and introduction of the complex variable U longitudinal vibrations, this system of equations is solved approximately by that method for boundary conditions

depending on the problem. Both the general solution U_{kn}^0 and the particular solution $U_{kn}^*(z, \bar{z})$ are obtained, the latter in the form of a double integral. The damping of vibrations, in terms of displacements as functions of time, has been analyzed numerically for a flat circular washer made of steel ($G = 0.8 \times 10^5$ MPa, $\nu = 0.25$, $\rho = 7.8$ kg/m³) with a 2:1 ratio of outside radius to inside radius, its inner contour under fluctuating uniformly distributed pressure and the outer contour free. Calculations made for three frequencies of pressure fluctuations (1250 s⁻¹, 2500 s⁻¹, 5000 s⁻¹) and for three values of the damping coefficient α ($0.002\rho\omega$, $0.02\rho\omega$, $0.2\rho\omega$) indicate that an increase of the pressure fluctuation frequency results in a higher initial energy, while an increase of the damping coefficient, too, results in a higher initial energy but also in a longer decay time and a lower final energy. Figures 2; references 1.

Action of Acoustic Wave on Set of Two Parallel Circular Cylinders in Ideal Fluid

917F0164G Kiev PRIKLADNAYA MEKHANIKA
in Russian No 1, Jan 91 pp 117-123

[Article by A.P. Zhuk, Institute of Mechanics, UkSSR Academy of Sciences, Kiev]

UDC 534.2:532

[Abstract] Action of an acoustic wave on two parallel free solid circular cylinders, one behind the other in the path of the wave, is analyzed by treating it as a problem of diffraction. The problem is formulated for a plane acoustic wave and two such cylinders with generally different radii $r_{1,2}$ in a boundless medium, a compressible ideal fluid. The problem is formulated in a rectangular global system of coordinates $Oxyz$ with the origin at a point half-way between the parallel axes of the two cylinders, the Ox axis in the direction of wave incidence crossing them at right angles, and the Oz axis running half-way between and parallel to them. The problem reduces to calculation of the velocity potential in the wave field, a mathematically linear problem of solving the linear wave equation, and to calculation of the radiation force. Solving the problem of diffraction for the incident primary wave with a given velocity potential requires calculating the velocity potential of the secondary wave field, which must satisfy the conditions of radiation at infinity and boundary conditions compatible with those for the primary field at the surfaces of both cylinders. This part of the problem is formulated in two cylindrical local systems of coordinates, one for each cylinder with the origin on its axis. It is solved, after separation of variables, in series of Hankel functions. Owing to symmetry with respect to the xOz plane, both cylinders oscillate with their velocity vectors in the Ox direction. The problem now reduces to an infinite series of linear algebraic equations solvable only by the truncation method. The radiation force on the cylinders is calculated by time-averaging the hydrodynamic force of the fluid medium on them. This force and the velocity

potential must be calculated with the same accuracy, including quadratic terms in parameters of the wave field. The action of an acoustic wave with a given amplitude ($0.9 \text{ cm}^2/\text{s}$ or given intensity (175.5 W/m^2 and frequency (8 kHz) on two cylinders in propanol (density $\rho_0 = 0.7854 \text{ g/cm}^3$) and the dependence of their attendant interaction on the distance between them are analyzed numerically according to this method. First are considered two cylinders with different radii ($r_1 = 1.3r_2$) in two configurations: smaller cylinder behind the larger and larger cylinder behind the smaller. The dependence of the radiation force at each cylinder on that distance between them is found to follow a slightly different trend in each case, evidently owing to different distributions of the secondary wave field. A larger radiation force is found to be always acting on the larger cylinder and the radiation force acting on the second cylinder, larger or smaller, to be equal to the radiation force acting on it if there were no other cylinder before it. The first cylinder thus does not influence the second one, which is consistent with the fact that reflected acoustic energy propagates in the opposite direction. Cylinders with equal radii are found to approach each other, faster or slower depending on the magnitude of the parameter kr (k -wave number. Calculations for this special case were made assuming an $L/r = 4$ length-to-radius ratio. The difference between the radiation forces acting on the two cylinders and causing them to approach each other does, moreover, becomes larger with higher frequency of the incident acoustic wave. Figures 5; references 5.

Resonance Dynamics of Vessel With Liquid Mounted on Vibration Dampers

917F0164F Kiev PRIKLADNAYA MEKHANIKA
in Russian No 1, Jan 91 pp 109-117

[Article by G.N. Puchka and V.V. Kholopova, Institute of Mechanics, UkSSR Academy of Sciences, Kiev]

UDC 629.78

[Abstract] The response of a cylindrical vessel with liquid mounted on stationary elastic vibration dampers to a periodic external excitation is analyzed for the important practical case of motion in a field of linear potential forces, i.e., where nonlinear effects of inertia dominate over nonlinear effects of elasticity. The equations which describe the resulting oscillations of the vessel and the free liquid surface are derived from the Hamilton-Ostrogradskiy principle of least action and formulated in two Cartesian systems of coordinates, one of them "absolutely" stationary ($O^*X^*Y^*Z^*$) and one rigidly affixed to the vessel (OX axis vertical and coinciding with cylinder axis). The height of the liquid column is assumed to be smaller than the height of the cylinder (vessel not full) but equal to or larger than its radius. For a determination of the velocity potential in the liquid, the boundary-value problem for the applicable equations of motion can then be solved by Narimanov's method (G.S. Narimanov, PRIKLADNAYA

MATEMATIKA I MEKHANIKA Vol 75, 21, No 4). The vessel is free to move in both orthogonal horizontal OY and OZ directions. As to oscillations of the free liquid surface, the first two antisymmetric modes (f_p and f_r) are most significant in terms of energy content and only they are being considered. The system of equations of motion is resolved with respect to higher-order derivatives, third-order derivatives of motion parameters having been retained in it, for subsequent analysis of the vessel-liquid dynamics by the method of averaging. A change from the natural space coordinates Y, Z to quasi-normal ones $Y = x_1 + x_2$, $p = \gamma_1 x_1 + \gamma_2 x_2$ and $Z = x_3 + x_4$, $r = \gamma_3 x_3 + \gamma_4 x_4$ facilitates determination of the four natural frequencies $\omega_{1,2}$ in the two directions in the XOY plane and $\omega_{3,4}$ in the two directions in the XOZ plane. The system of equations of motion is resolved with respect to higher-order derivatives, the third-order derivatives of the motion parameters having been retained, for subsequent analysis of the vessel-liquid dynamics by the method of averaging. The conditions are thus established under which the two antisymmetric oscillation modes of the free liquid surface will appear and when oscillations of the vessel-liquid system in one plane only, the XOY plane of excitation, will change to oscillations in both XOY and XOZ planes. Special attention is paid to such compound oscillations in two orthogonal planes in the special case of an attendant internal resonance, with two pairs of equal natural frequencies $\omega_1 = \omega_3$ and $\omega_2 = \omega_4$, in addition to resonance excitation at a frequency $\omega \approx \omega_1 = \omega_3$ or $\omega_2 = \omega_4$. Figures 3; references 6.

Stability Theory for Motion of Triple-Unit Vehicles on Tires

917F0164E Kiev PRIKLADNAYA MEKHANIKA
in Russian No 1, Jan 91 pp 96-103

[Article by L.G. Lobas, V.P. Sakhno, and T.I. Tarnopol'skaya, Institute of Mechanics, UkSSR Academy of Sciences, Kiev, and Kiev Institute of Automobile Roads]

UDC 531.384:629.114

[Abstract] A mathematical model describing plane-parallel motion of triple-unit motor vehicles on tires is constructed for a stability analysis of that motion. As a specific example is considered a tandem trailer truck consisting of a tractor and two trailers, the first one being a platform without wheels which clears the road surface. Change from Cartesian space coordinates x, y of the inertial system to quasi-velocity coordinates $v = (dx/dt)\cos\delta + (dy/dt)\sin\delta$, $u = -(x/dt)\sin\delta + (y/dt)\cos\delta$ (δ -course angle of tractor) makes it possible, by virtue of the laws kinematics, to separate the variables in the equations of dynamics and thus split the system of these equations into two lower-order subsystems of two equations for forces and moments. In addition to the driving and reaction moments there are also included here damping and restoring moments which viscoelastic supporting-and-coupling devices produce, these moments depending on the trailer folding angles $\varphi_{1,2}$ and their

time derivatives. The resulting linear combination of four equations is reformulated in variations, for a stability analysis of uniform rectilinear motion describable by an inertia matrix in accordance with the single-track model of a tandem trailer truck which in this case includes two supporting- and-coupling devices. An analytical solution for the critical velocity is supplemented with numerical data pertaining to typical such trailer truck. The critical velocity is shown to depend on the distance from the tractor-platform coupling point to the center of mass of the tractor, becoming infinitely high when that distance is the critical one and becoming zero when that distance is smaller. Figures 4; references 12.

Vibrations of Reflector Antenna Shells Under Vibratory Excitation

917F0164D Kiev PRIKLADNAYA MEKHANIKA
in Russian No 1, Jan 91 pp 64-71

[Article by V.S. Gudramovich, N.G. Baranov, N.A. Kononov, and I.M. Maytala, Institute of Engineering Mechanics, UkSSR Academy of Sciences, Dnepropetrovsk]

UDC 538:539.2:773.5.004

[Abstract] An experimental study of reflector shells for large antennas was made concerning their vibrations under vibratory loads, such loads acting during seismic activity on ground antennas as well as on spaceborne antennas while the spacecraft is put in orbit by a rocket. A paraboloidal 0.35 mm thick shell serving as the larger reflector of a two-reflector antenna, made of nickel (modulus of elasticity $E = 7 \times 10^4$ MPa, tensile strength 140 MPa, 0.2 % yield point 175 MPa), was tested in both vertical and horizontal positions on a VEDS-1500 electrodynamic exciter. The length of the shell was 0.44 m and the radius of its base was 0.78 m. The shell was tested in a reinforcing hoop and without it, the cross-section of the hoop being 0.0115 m^2 and also without large. For a determination of its amplitude-frequency characteristics and vibration resistance, it was tested over the 5-4000 Hz frequency range under 6-12 g accelerations from 0.6 g to 12 g. The vibration amplitudes were measured with five ANS-14 piezoelectric accelerometers spaced 0.180 m apart on a flange made of Al-Mg(6M) aluminum alloy and mounted around the shell at the 0.231 m radius of the latter. The frequency marker, developed at the Institute of Engineering Mechanics, was a device consisting of two pairs of stationary light-emitting photodiodes and a rotating disk with two rows of holes coupled to an excitation frequency indicator. The electric output signals from those accelerators were recorded on an NO-67 magnetograph and also on an NO-45 loop oscillograph, with the AGK-2 harmonic analyzer developed at the Institute of Engineering Mechanics as matching device. The vibration modes of the shell with and without hoop at two resonance frequencies, 9 Hz and 140 Hz, were photographed with a "Gladiolus-1" camera at the maximum rate of

240 frames/s with a 90° shutter so as to allow 1/190 s exposure time, and recorded on KN-4 film. The results of this study indicate, most importantly, the effectiveness of stiffening such an antenna reflector shell. Figures 5; tables 1; references 4.

Design of Viscoelastic Thin-Walled Shells Considering Their Damageability

917F0164C Kiev PRIKLADNAYA MEKHANIKA
in Russian No 1, Jan 91 pp 55-61

[Article by Ya.A. Eyubov, Azerbaijan Institute of Structural Engineering, Baku]

UDC 539.3

[Abstract] A method of designing viscoelastic thin-walled shells with consideration of their damageability and geometrical nonlinearity is developed by application of the variational principle to calculation of stresses and strains, this principle being derived from the one for a three-dimensional body. Solution of the corresponding boundary-value problem is difficult, because the constraint on the solution is the differential equation of damage process kinetics and the functional depends on the damageability parameter. Since only a limited number of coordinate functions will satisfy this constraining differential equation of kinetics, an exact solution of it is waved by replacing it with an approximate integral relation. The functional, whose Euler equation contains the kinetics of damage, thus becomes one of the mixed kind. The nonlinear problem of viscoelasticity for given boundary condition and then for the initial conditions is solved accordingly, by the Ritz method. As an example is considered a cylindrical viscoelastic shell, a pipe, hinge-supported at both end and under an internal pressure uniformly distributed over the lateral surface. A numerical analysis of the solution to the corresponding Cauchy problem indicates that increasing the wall thickness of such a shell will lengthen the critical time till fracture occurs, but not proportionally. Figures 2; references 4.

Use of Acoustoelasticity Theory of Rayleigh Surface Waves for Determination of Stresses in Solid Bodies

917F0164B Kiev PRIKLADNAYA MEKHANIKA
in Russian No 1, Jan 91 pp 44-49

[Article by A.A. Chernoochenko, F.G. Makhort, and O.I. Gushcha, Institute of Mechanics and Institute of Electric Welding imeni Ye.O. Paton, UkSSR Academy of Sciences, Kiev]

UDC 539.3.:620.179.16

[Abstract] Biaxial stresses which electric welding produces in the surface layer of an elastic and initially isotropic solid body are calculated according to the acoustoelasticity

theory of Rayleigh surface waves in the linear approximation. The sum and the difference of principal stresses $\sigma_{11} + \sigma_{33}$ and $\sigma_{11} - \sigma_{33}$ are first expressed in terms of the velocities of those waves propagating through that layer along the principal axes OX_1 and OX_2 . For a better interpretation of experimental data, they are then expressed in terms of the recirculation frequencies of ultrasonic waves or pulses used for measurements by the recently developed acoustic method. In an experiment with two disks, one of D16 aluminum alloy 35 mm thick with a 180 mm in diameter and one of 10Mn2VB alloy steel 15 mm thick with a 120 mm diameter, biaxial stresses in them were produced by diametral compression along the vertical OX_1 axis with a constant load of 100 kN (aluminum alloy) and 400 kN (steel) respectively. Stresses were measured along the horizontal diameter on the OX_3 axis at various distances from the center. Ultrasonic surface waves in these disks were transmitted and received by a pair of piezoelectric transducers, changes in the recirculation frequencies during the compression process being recorded by instrument in the 10^{-4} -error accuracy class. Each transducer consisted of two 4 mm thick and 10 mm wide plates made of TsS-19 (Sr zirconate-titanate) piezoceramic, rigidly joined to form a "wedge" with a resonance frequency of 3 MHz. In a separate test rectangular plates 20 mm thick, 50 mm wide, and 70 mm long were compressed lengthwise while the recirculation frequencies of ultrasonic surface waves were measured along and across the plates. The results validate this method of stress measurement. It therefore was used for measurement of residual stresses in an 8 mm thick, 70 mm wide, and 310 mm long rectangular plate hard-faced by electric welding, for calibration of the proportionality factors in the theoretical formulas. Figures 3; tables 1; references 11.

Stressed and Strained State of Half-Space Due to Translatory Motion and Rotation of Partly Embedded Rigid Ball Partly

917F0164A Kiev PRIKLADNAYA MEKHANIKA
in Russian No 1, Jan 91 pp 24-31

[Article by I.K. Senchenkov, V.G. Savchenko, O.P. Chervinko, and V.I. Bobyr, Institute of Mechanics, UkSSR Academy of Sciences, Kiev]

UDC 539.3.01

[Abstract] A stress and strain analysis is performed for a composite material which consists of an elastic binder matrix with fine abrasive filler grains moving in it, and the integral stiffness characteristics of such a system are evaluated in connection with the use of such materials for cutting tools. The model for this analysis is a perfectly hard spherical grain only partly embedded in an only slightly deformable isotropic and linearly elastic matrix occupying a half-space. The grain rotates about its two axes respectively parallel and perpendicular to the matrix surface, while it also moves in a straight line but so constrained that its embedment depth remains constant. Interaction with neighboring grains is assumed

to be negligible. The depth of grain embedment in the matrix is characterized by the ratio $\Delta = \Delta'/R_0$ (R_0 - radius of grain), $0 < \Delta < 2$ ($\Delta = 0$ corresponding to a grain on the matrix surface and $\Delta = 2$ corresponding to a grain completely under the matrix surface). The motion of a spherical grain is treated as that of a solid body under a force $N = (N_x, N_y, N_z)$ and a moment $M = (M_x, M_y, M_z)$. In view of the axial symmetry of the problem, a system of cylindrical coordinates is added for displacements. The equations of balance for the components of force and momentum are then solved for boundary conditions of zero displacements on the matrix surface and zero stresses on the grain surface. The nonzero boundary conditions for strains are stipulated on points of the circular corner along which the grain surface intersects the matrix surface. The problem is solved by the method of finite elements, its solution being sought in the form of a trigonometric series with respect to the angular circumferential coordinate. A numerical analysis of the solution reveals how not only the stresses and the strains in the matrix but also of the elements of its stiffness matrix depend on the grain embedment depth, including their asymptotic behavior as the that depth tends to infinity. Figures 5; references 5.

Stressed State of Noncircular Thick-Walled Cylinders Depending on Indicators of Load Nonuniformity Along Generatrix and Directrix

917F0217A Kiev PRIKLADNAYA MEKHANIKA
in Russian No 3, Mar 91 pp 12-18

[Article by Ya.M. Grigorenko, G.G. Vlaykov, and S.N. Shevchenko, Institute of Mechanics, UkSSR Academy of Sciences, Kiev]

UDC 539.3

[Abstract] The stressed state of noncircular thick-walled hollow cylinders is analyzed for its dependence on the degree of load nonuniformity along the generatrix and the directrix. The analysis is premised on the three-dimensional theory of elasticity. A noncircular cylinder is placed in an orthogonal curvilinear system of coordinates s, t, γ (coordinates $s = \text{const}$ and $t = \text{const}$ on lines of principal curvatures of the median surface, representing families of generatrices and directrices respectively, coordinate γ in direction normal to the median surface). The problem is formulated as a system of six partial differential equations $\delta V/\tau = F(V, \delta V/\delta s, \delta V/\delta \gamma, \delta^2 V/\delta s^2, \delta^2 V/\delta \gamma^2, \delta^2 V/\delta s \delta \gamma, P, T)$ (P - load vector, T - temperature field) which has been resolved for the first derivatives of its components with respect to the t -coordinate. Satisfying the conditions of periodicity or symmetry of the stressed state will reduce solution of the problem for closed cylinders to solution of the problem for open ones, these conditions to be satisfied by a compatible combination of sufficiently smooth functions defining the boundary conditions at sections of a cylinder bounded by its directrix $t = \text{const}$. Boundary conditions at lateral surfaces are stipulated in terms of stresses. The problem is solved in the region $0 \leq$

$s \leq L$, $t_0 \leq t \leq t_N$, $-H/2 \leq \gamma \leq H/2$ ($H_1 = 1$, $H_2 = R$, $h_3 = 1$, R_c - radius of curvature of directrix which defines the median surface). The problem is solved by combining separation of variables with subsequent direct and discrete orthogonalization. First the dimensionality of that system of equations is lowered by expansion of given and sought functions into Fourier series in the s -coordinate. Separation of variables then reduces the three-dimensional problem to a series of two-dimensional ones for each Fourier harmonic. This series of two-dimensional problems in s, γ coordinates is then, by the straight lines method, reduced to a one-dimensional boundary-value problem for an N^* -order system of ordinary differential equations ($N^* = 6n - 4$, n - number of points on the finite-differences approximation over the cylinder wall thickness) $dV^*/dt = A(t)V^* + B(t)$ where $A_1 V^*(t_0) = B_1$ and $A_2 V^*(t_N) = B_2$ ($A_{1,2}$ - rectangular $N^*/2 \times N^*$ matrices, $B(t)$ - given N^* -dimensional vector, $B_{1,2}$ - given $N^*/2$ -dimensional vectors). This equation can now be solved very accurately by the numerical method of discrete orthogonalization. This is demonstrated on hollow elliptical thick-walled cylinders. The perimeter of the median surface is equated to the circumference of a circle with a radius R and the cross-section is described by two parametric equations $x = b \cos \theta$, $z = a \sin \theta$ (a, b - semiaxes of the ellipse). The results indicate an interaction of loads non-uniformly distributed along the two coordinates s and t respectively. Figures 4; tables 2; references 5.

Solution of Problems Pertaining to Parametric Vibrations of Shells of Revolution by Method of Finite Elements

917F0217B Kiev PRIKLADNAYA MEKHANIKA
in Russian No 3, Mar 91 pp 32-37

[Article by A.T. Vasilenko, S.S. Kokoshin, and P.N. Cherinko, Institute of Mechanics, UkSSR Academy of Sciences, Kiev

UDC 539.3

[Abstract] Parametric vibrations of thin-walled shells of revolution with a uniform thickness are analyzed by the method of finite elements, the invariance property of this method making it possible to solve the problem of such vibrations for shells with essentially any geometrical and mechanical characteristics under any constraints and under any mechanical or thermal loads. As a specific example is considered a shell under a harmonic perturbation force. The functional of total potential energy for this problem consists of four terms, each a surface integral, two of them representing respectively the generalized strain energy in the perturbed state at the instant of stability loss and the strain energy during variation of displacements under constant stresses in the subcritical state. A third term representing kinetic energy is added and a fourth term representing work done by the load being subtracted. The relation between generalized strains ϵ and generalized displacements U is

expressed in the form $\epsilon = LU$ (L - matrix of differentiation operators). Following separation of variables for the displacement vector, the kinematic relations between strains ϵ and displacements of nodal points Δ_k are for each finite element are expressed in the form $\epsilon = B\Delta_k$ (B - matrix which includes the L matrix). Angular displacements ω are related to linear displacements U through a matrix L' of differentiation operators so that $\omega = L'U$ and to displacements of nodal points Δ_k through a matrix G (which includes the L' matrix) so that $\omega = G\Delta_k$. The expression for the potential energy of each finite element is then expressed in terms of Δ_k displacements rather than strains. The coefficients with which these displacements appear are the physical stiffness matrix, the geometrical stiffness matrix, the mass matrix, and the vector of generalized time-dependent actions (forces, moments) at nodal points. All three matrices, each a double integral, are evaluated numerically by the Gauss method. The condition of steadiness of these functionals with respect to Δ_k' (velocity) and Δ_k'' (acceleration) leads to two systems of algebraic resolvent equations $\det | \dots | = 0$ and thus to an eigenvalue problem for two systems of equations. In the absence of external loads and for correspondingly zero initial stresses, moreover, the problem reduces to natural vibrations of a shell. Otherwise the problem is characterized by involving two parameters, namely initial stresses as load parameter in addition to frequency. It can be solved by inverse iterations with the aid of Rayleigh's relations. The method was applied to two specific problems, one a test problem with a known analytical solution and one which had already had been solved numerically by the method of discrete orthogonalization. The first problem was to calculate, in accordance with the classical theory of shells, the spectrum of lower-order natural vibrations of a closed cylindrical one freely supported at both ends. The second problem was to analyze parametric vibrations of an isotropic cylindrical shell fixed at one end in a sliding constraint at the other. Tables 2, references 12.

Axisymmetric Problem of Impact of Solid Body against Thin Membrane Floating on Compressible Fluid Half-Space

917F0217C Kiev PRIKLADNAYA MEKHANIKA
in Russian No 3, Mar 91 pp 38-45

[Article by V.D. Kubenko, Institute of Mechanics, UkSSR Academy of Sciences, and V.V. Gavrilenko, Institute of Automobile Roads, Kiev]

UDC 533.6.013.42

[Abstract] Impact of an axisymmetric blunt solid body of otherwise arbitrary shape against a thin circular membrane with a finite radius floating on the boundary of a compressible fluid which occupies a half-space is considered, the body having moved in the direction of its axis of symmetry and approached the membrane normally to its surface before striking it at the center. The fluid is

assumed to be a weightless barotropic ideally compressible one. The problem is formulated in the linear approximation, with corresponding constraints on the velocity $v_0(t)$ of the body and on the deflection w^* of the median surface at its center after impact at time $t = 0$: $v_0(t) < c$ (speed of sound in the fluid) and $w^* < R$ (radius of membrane). The shape of the body surface at any instant after impact is described by the equation $z = \Phi(t, \theta)$ (θ -polar angle from axis of body and membrane symmetry to membrane-fluid contact circle, Φ -slightly curving piecewise-smooth even function). The wave function for the fluid and the classical equations of dynamics for the membrane are modified so that their solutions can be obtained in the form of series in the same system of Legendre polynomials, while the boundary conditions are linearized and then reduced to those at the quiescent fluid surface. This is made possible by identifying the linear coordinates along the body, membrane, and fluid surfaces for the early stage of body-membrane-fluid interaction. In order to solve the problem then, it is necessary to first solve two auxiliary ones. One of them is establishing the relation between the strain rate of the fluid surface $V(t, \theta)$ and the hydrodynamic pressure $p(t, \theta)$ on it, which is done by Laplace transformation of both and subsequent expansion of their Laplace transforms into a Fourier series in Legendre polynomials. The other problem is establishing the relation between both deflection $w(t, \theta)$ and rate of deflection $dw(t, \theta)/dt$ and the pressure $p(t, \theta)$, which is done analogously and by applying the convolution theorem for two original functions. On the basis of this theoretical model, the problem of impact was solved numerically for a rigid sphere and a thin steel membrane on water. Figures 4; references 8.

Viscoelastic State of Cylindrical Triple-Layer Shell Under Pulsed Heat or Force Load

917F0217D Kiev PRIKLADNAYA MEKHANIKA
in Russian No 3, Mar 91 pp 46-52

[Article by E.I. Starovoytov and S.A. Vorobyev, Belorussian Institute of Railroad Transportation Engineers]

UDC 539.3

[Abstract] A not so flat cylindrical shell with a carrier-filler-carrier structure and an asymmetrically nonuniform thickness under a pulsed heat or force load is considered, the material of the filler being different than the material of the two carriers but both materials being isotropic. Both materials are characterized by elasticity of volume changes and a linear viscoelastic lag in shear. The behavior of the two outer layers conforms to the Kirchhoff-Love hypotheses and that of the inner one conforms to the exact theory of elasticity in the linear approximation of displacements from the transverse coordinate. The boundary conditions at the contact surfaces are continuity of displacements. Strains are assumed to be small. The problem is formulated in a cylindrical system of coordinates and solved for tangential displacements and normal ones (deflections) of

points on the median surface of each layer. It is solved by application of the Hamilton-Ostrogradskiy principle, which leads to a system of six integrodifferential equations describing the motion of such a shell. This system of equations is solved by the Bubnov-Galerkin method, first for the quasi-static problem as a test case. In this case it reduces to a system of Volterra equations of the second kind, after the inertia terms have been discarded on account of their smallness. The solution of this problem establishes the confidence level for analysis of the shell dynamics, that problem being solved by the numerical Denisenko-Yanovich method (N.V. Denisenko and L.A. Yanovich, DIFFERENTIAL'NYYE URAVNIENIYA Vol 19 No 5, 1983) for boundary conditions of free supports at both ends. The method is based on reversibility of the differential operator associated with three constant diagonal matrices μ , κ , p . As a first example is considered a normally incident uniform thermal flux heating the shell continuously from time $t = 0$ on. The transient temperature field nonuniformly distributed over the stack thickness is then calculated according to Starovoytov's formula, disregarding the curvature of layers. As a second example is considered heating of the shell for a certain time interval only and subsequent stabilization of the temperature field. Creep is included in numerical calculations for carrier layers of D16T duralumin and a filler layer of teflon (polytetrafluoroethylene). As a third example is considered an impulse $A\delta(t)$ of pressure (δ -Dirac's delta-function) loading the shell axisymmetrically. Figures 4; tables 1; references 9.

Elastic Displacements Vector of Thin Spherical Shell

917F0217E Kiev PRIKLADNAYA MEKHANIKA
in Russian No 3, Mar 91 pp 63-69

[Article by V.A. Merkulov, Volgograd Institute of Construction Engineering]

UDC 539.3:534.1

[Abstract] Considering that the displacement vector of a closed thin spherical shell needs to be known for a precise analysis of its natural vibrations, its elastic displacements vector U and elastic rotations vector Γ of the median surface are calculated on the basis of a linear displacement profile across the shell wall thickness in accordance with the Kirchhoff-Love hypotheses. This profile is described in the form of the vector relation $U_z = U + z\Gamma \times e_n$ (U_z - displacements vector, z - thickness coordinate, x - vector product, e_n - normal unit vector). To this relation are added relations describing the linear dependence of strain components on the distance from the median surface, these relations corresponding to Love's equations of state. Differentiation of the generalized displacement vector with respect to each of the two geographical coordinates generates a system of two differential equations relating the two derivatives to the radius of the median surface of the shell in terms of

strains and angular displacements for the vibration mode vector V_z . Equality of its mixed derivatives being the condition for integrability of that system of equations, they together with the relations describing linear strain profiles across the shell wall thickness yield relations between angular displacements and strains. These relations are, in accordance with Love's equations of state, transformed into a system of three equations of balance of forces (normal forces $T_1 + T_2 = T$, shearing force S) and moments (bending moments $M_1 + M_2 = M$, twisting moment H) which in turn yields a system of three resolvent equations for the three u, v, w displacements and then a system of two equations for natural frequencies: one for the frequencies of vibrations of an element of the median surface about the normal to it and one for two series of frequencies of conjugate radial-tangential vibrations. Both series of frequencies ω_n are then calculated by Novichkov's method (Yu.N. Novichkov, Handbook: "Vibrations in Engineering", Izd. Mashinostroyeniye, 1978). One series is $[q <] \infty$ with $n = 0, 1, 2, \dots$, the $n = 0$ mode being the tension-compression mode of equal purely radial displacements of points of the median surface. The highest frequencies of tangential tensile and shearing vibrations have been calculated according to the Novichkov's formula with $A_n + (A_n - 4B_n)^{1/2}$ in the numerator for this series. The other series is ω_n with $n = 1, 2, \dots$ and no $n = 0$ mode. The lowest frequencies of radial tensile and shearing vibrations have been calculated according to Novichkov's formula with $A_n - (A_n - 4N_n)^{1/2}$ in the numerator for this series. References 11.

Numerical Analysis of Statics of Smooth and Discretely Reinforced Shells Under Combined Flexural and Axial Load

917F0217F Kiev PRIKLADNAYA MEKHANIKA
in Russian No 3, Mar 91 pp 69-75

[Article by V.P. Maksimenko and N.V. Kovalchuk, Institute of Mechanics, UkSSR Academy of Sciences, Kiev]

UDC 539.3

[Abstract] The static stressed and strained state of closed thin-walled circular cylindrical shells discretely reinforced by an orthogonal grid of hoops and stringers, stiffer rings at both ends, under a combined axial and flexural load is analyzed following a solution of both Vlasov's equation of balance and compatibility equation for strains (V.Z. Vlasov, "General Theory of Shells and Its Engineering Application", Gostekhizdat, 1949). The load at the upper end of the shell is an axial force q uniformly distributed over the base circle and a concentrated radial transverse force Q applied to the top ring. The load at the lower end of the shell is four axial forces P distributed each over one of the four $s = \pi R/6$ long arcs (R - radius of shell) symmetrically spaced around the base circle. These are the reactions of four mounts on which the shell rests, spaced symmetrically 90° apart under the

lower base either so that one pair lies on the diameter parallel to the line of action of force Q and the other pair lies on the diameter in quadrature or so that both pairs lie on diameters at 45° to the line of action of force Q . The problem is for each case split into two separate ones, for the transverse load and for the axial load respectively, this being permissible by virtue of the principle of independent action of forces. The first problem has one plane of symmetry and one plane of antisymmetry. The second problem has only several planes of symmetry. Both problems are also solved for smooth shells, as a basis for evaluating the effectiveness of reinforcement. The equations of balance and compatibility, each with four finite series on the left-hand side, are reduced to a system of linear algebraic equations for numerical solution by the Gauss method. As an example is considered a shell made of Al-Mg(6M) aluminum alloy (radius $R = 20$ cm, length $L = 5\pi R/8$, wall thickness $t = R/400$) with 32 stringers, 4 hoops, and two end rings. The results are compared with experimental data, tests having been performed on 42 such shells with a different Q/P load ratio for each. Figures 5; tables 3; references 7.

Supercritical Deformation of Real Cylindrical Shells Under External Pressure and Estimation of Their Stability

917F0217G Kiev PRIKLADNAYA MEKHANIKA
in Russian No 3, Mar 91 pp 76-83

[Article by A.Yu. Yevkin and V.L. Krasovskiy, Dnepropetrovsk Institute of Construction Engineering]

UDC 539.3

[Abstract] Formulas for the sensitivity of shells to perturbations based on an analysis of supercritical deformation according to Coyter's [transliteration] theory were on checked out experimentally on real cylindrical shells under external pressure for a verification of stability estimates. Special shells for this experiment were produced from strips of normalized Cr18Ni9 stainless steel by spot welding them into cylinders with an $R = 71.5$ mm inside radius, an active length $L = 2.0R$, and a wall thickness $t = 0.00375R$. Each shell was hermetically closed at both ends so as to prevent leaks into the cavity and ensure constancy of the constraints, which approximated those of free support. External loading was effected by sucking air out of the cavity. In the first experiment preliminary depressions simulating local imperfections were produced either so as to leave no residual stresses or so as to conform to the stable supercritical configuration with one local depression. In the second experiment preliminary protrusions simulating local imperfections were produced by buckling under various under various lower pressures. For a second evaluation of the effect of subcritical regular imperfections "resonating" with the supercritical shell configurations on the magnitude of the critical pressure, the results of this experiment are interpreted by considering the equilibrium position of a shell after large deformation. Theoretically this problem is

solved on the basis of nonlinear equations in Volmir's mixed theory of shells (A.S. Volmir, "Stability of Deformable Systems", Izd. Nauka, 1967). It is solved by the asymptotic method using Pade's approximations. A comparison of stability estimates according to this and Coyter's method indicates that the latter are erroneous in the case of large deformation. This method therefore is preferable when initial deflection must be taken into account, which can be done by expressing the dependence of the load parameter on the total deflection in the form a complete quadratic polynomial. Figures 5; references 12.

Vibrations of Triple-Layer Plate of Finite Dimensions in Contact With Liquid

917F0217H Kiev PRIKLADNAYA MEKHANIKA
in Russian No 3, Mar 91 pp 88-93

[Article by S.N. Beshenkov and T.D. Volkova, Zaporozhye University]

UDC 539.3:534.1

[Abstract] A triple-layer plate of finite dimensions fastened to an infinitely stiff frame and floating on the surface of a liquid which occupies a half-space is considered, its forced harmonic vibrations being analyzed in two ways. First they are analyzed on the basis of the simplified theory for a sheath-filler-sheath plate which disregards transverse compressibility of the filler in accordance with the broken-line hypothesis. Its deformation is described by the Goloskokov-Filippov system of three equations (Ye.G. Goloskokov and A.P. Filippov, "Nonsteady Vibrations of Deformable Systems", Izd. Naukova Dumka, 1977) in deflection w of the plate, tangential displacement u of the median plane of the filler, and angular displacement ω of its plane sections under a net load equal to the difference $q - p$ between excitation force and reaction of the liquid, the time factor $e^{i\omega t}$ being omitted. This system of equations is solved for boundary conditions of free support at the ends with w , u , ω as well as q and p expressed in the form of infinite Fourier series. The longitudinal profile of the acoustic pressure, reaction of the liquid, is approximated as a piecewise-linear one and its unknown magnitude of that pressure at the nodes is calculated using the Huygens integral of plate deflections. Insertion of w , u , and ω into that integral then leads to a system of algebraic equations for reaction of the liquid at the nodes. The problem is also solved on the basis of the refined theory, taking into account motion of the filler and describing it in accordance with the dynamic theory of elasticity: $c_1^2 \text{grad div } r - c_2^2 \text{curl curl } r + \omega^2 r = 0$ (c_1 - velocities of longitudinal and transverse waves in filler, r - displacement vector, ω - vibration frequency). Normal and shearing stresses in the filler along its boundaries with the two sheaths are calculated in accordance with Hooke's law. The continuity condition for displacements in the plate then yields the deflections of the lower sheath in contact with the liquid. The acoustic pressure of the

liquid is calculated using the Huygens integral of these deflections, which again leads to a system of algebraic equations for reaction of the liquid at the nodes. Both methods were applied to two plates with a $2h = 2$ mm thick filler of a material with a modulus of elasticity $E = 5 \times 10^7$ N/m² in one plate between two aluminum sheaths of the same thickness $t = 3$ mm (symmetric structure) and in one plate between two aluminum sheaths of unequal thicknesses $t_1 = 5$ mm, $t_2 = 1$ mm (asymmetric structure), both plates being excited by a linear force $F = 1000t(x - L/2)$ N/m (L - length of plate). Calculations were made for a numerical evaluation of the dependence of the plate deflection at its center and of the reaction of the liquid (acoustic pressure) at that point on the excitation frequency. Both deflection and pressure were treated as complex quantities, their real and imaginary parts being calculated separately. Deflection of the symmetric plate structure and acoustic pressure on it were found to have analogous frequency characteristics, with maximum imaginary part and zero-crossover of the real part at the same resonance frequencies (150 s⁻¹ and 1410 s). The results of calculations for the asymmetric plate structure reveal the effect of that asymmetry on the two frequency characteristics. The results of calculations by the second method, moreover, reveal the effect of compressibility of the filler. Figures 3; references 8.

Interaction of Acoustic Wave and Two Parallel Cylinders in Viscous Fluid

917F0217I Kiev PRIKLADNAYA MEKHANIKA
in Russian No 3, Mar 91 pp 108-115

[Article by A.P. Zhuk, Institute of Mechanics, UkSSR Academy of Sciences, Kiev]

UDC 532.516:539.376

[Abstract] Interaction of an acoustic wave and two parallel free circular cylinders with generally different radii $r_{1,2}$, one behind the other in the path of the wave, in a viscous compressible fluid is treated as a problem of diffraction. The problem is formulated in a rectangular global system of coordinates for the velocity potential of the wave field and in two cylindrical local systems of coordinates, one for each cylinder with the origin on its axis for the two successive diffractions of the incident primary acoustic wave. The rectangular system of coordinates, its origin at a point O half-way between the parallel axes of the two cylinders, is oriented with the Ox axis in the direction of wave incidence crossing them at right angles and the Oz axis running half-way between and parallel to them. The mean force of the fluid on each cylinder is defined as a surface integral, the product of the stress tensor in the fluid by the normal unit vector being integrated over the surface of each cylinder, and is calculated by time-averaging this integral. The mean force acting along the Ox axis was calculated numerically for two cylinders with equal radii $R = 0.1$ cm in propanol (density $\rho_0 = 0.7845$ g/cm³), $L = 1$ cm apart, and an acoustic wave of 175.5 W/m² intensity. The results

indicate that the mean force on each cylinder depends on the wave frequency and on the density ρ of its material. When its density is lower than that of the fluid and the cylinders float, then the first cylinder influences the behavior of the second more than the second cylinder influences the behavior of the first. In both cases of $\rho_0 > \rho$ and $\rho_0 < \rho$ the two mean forces acting on each cylinder (force of the incident wave and force of the wave reflected by the other cylinder) act in opposite directions, the two cylinders attracting each other in the first case and repelling each other in the second case. As the viscosity of the fluid decreases with rising temperature, moreover, an acoustic wave produces a smaller mean force on the cylinders. Figures 5; references 6.

Design of Framed Shells of Intricate Shapes for Internal Pressure Load

917F0217J Kiev PRIKLADNAYA MEKHANIKA
in Russian No 1, Mar 91 pp 119-124

[Article by V.V. Kuznetsov and Yu.V. Soynikov, Siberian Scientific Research Institute of Aviation, Novosibirsk]

UDC 539.3

[Abstract] An economical algorithm is proposed for design calculation of the stressed and strained state of linear shells in reinforcing frames, geometrically linear structures, taking into account deflections of the joints with the reinforcing members. It is based on the method of finite elements using the Hess matrix H^{Π} of second derivatives of the potential energy with respect to generalized coordinates, triangular finite elements are selected for a thin shell. Their generalized elastic displacements vector is defined in terms of the strain tensor of their median surfaces and the generalized q -coordinates vector q is defined in terms both linear and angular displacements. For finite elements of the reinforcement members both vectors are defined analogously, but referring to corners of a finite element and disregarding the nonlinear terms. The generalized q -coordinates q is determined from the system of equations $H^{\Pi}q = R$ (R - vector of external forces). The algorithm has been programmed for a BESM-6 high-speed computer. It was tested on shells of noncanonical shapes conforming to

the Kirchhoff-Love hypotheses under an internal pressure load and the results compared with experimental data, the agreement being quite satisfactory. Figures 5; references 7.

Experimental Stability Study of Nonconservative Systems

917F0217K Kiev PRIKLADNAYA MEKHANIKA
in Russian No 3, Mar 91 pp 124-127

[Article by M.Kh. Mullagulov, Ufa Institute of Aviation]

UDC 539.3

[Abstract] The test stand built for experimental stability study of nonconservative systems where the pressure of the air jet discharged by a nozzle at the free end of a uniform cantilever beam serves as the tracking compression force P on this beam was used for determining the critical length L of the beam according to the $P_{cr} = 14.8EJ_{min}/L^2$ criterion rather than the $P_{cr} = 20.2EJ_{min}/L^2$ based on the dynamic criterion of stability. The tracking force in this test stand is produced by a propeller driven by a small variable-speed 0-600 rpm 1.47 kW electric d.c. aircraft motor weighing 2.6 kg. The tested beam, a rectangular bar of quenched 25CrMnSiN₂ steel, is rigidly clamped at one end to the test stand table in a horizontally cantilever position. The motor with an aerodynamically streamlined propeller on the shaft extension is suspended on a thread so as to face the free end of the beam rather than being attached to it. This arrangement eliminates deflection of the beam. The twisting moment, which the propeller produces in addition to the axial tracking compression force, is absorbed by a carriage also mounted at this end of the beam and consisting of a two slotted guide bars for a steel ball each inside a yoke. The tracking force can be varied by varying the voltage at the motor terminals. The beam can thus be subjected to a force from 0 to 20 N continuously and up to 30 N for a short time. One drawback of the test stand are small vibrations, due to some rotor and propeller unbalance, these vibrations becoming larger and their effect on the test results becoming more appreciable with increasing motor speed. Tests were performed during the 1986-89 period by many researchers including M.Kh. Mullagulov, on four beams 70, 80, 90, 100 cm long with a rectangular 0.97 cm x 3.94 cm cross-section. The beams were also tested for stability under a tracking tension force, attempts to induce instability in the form of either whip or flutter not having been successful. Figures 2; tables 1; references 5.

Design of Closed-Loop for Control of Robot With Torque Motors

917F0163A Leningrad IZVESTIYA VYSSHIKH
UCHEBNYKH ZAVEDENIY: PRIBOROSTROYENIYE
in Russian No 12, Dec 90 pp 15-20

[Article by A.V. Timofeyev, V.A. Baykalov, and I.R. Fomina, Leningrad Institute of Aircraft Instrument Design]

UDC 62.50

[Abstract] Automatic control of the manipulator in robots with torque motors is synthesized on the basis of

the Lagrangevector differential equation describing the manipulator dynamics, proportional-differential regulators being considered for this system. Stability of regulator operation has been selected as the criterion for design and selection of the drive for each degree of freedom. Accuracy and response speed of the control system are then estimated for design review. The calculations have been programmed on a Standard System 1045 computer in various languages (FORTRAN, PASCAL, PL/1) for educational and research purposes. A typical menu is shown for computer-aided design of such an automatic control for SKARA robots. Tables 1; references 5.

NTIS
ATTN: PROCESS 103
5285 PORT ROYAL RD
SPRINGFIELD, VA

2

22161

This is a U.S. Government publication. Its contents in no way represent the policies, views, or attitudes of the U.S. Government. Users of this publication may cite FBIS or JPRS provided they do so in a manner clearly identifying them as the secondary source.

Foreign Broadcast Information Service (FBIS) and Joint Publications Research Service (JPRS) publications contain political, military, economic, environmental, and sociological news, commentary, and other information, as well as scientific and technical data and reports. All information has been obtained from foreign radio and television broadcasts, news agency transmissions, newspapers, books, and periodicals. Items generally are processed from the first or best available sources. It should not be inferred that they have been disseminated only in the medium, in the language, or to the area indicated. Items from foreign language sources are translated; those from English-language sources are transcribed. Except for excluding certain diacritics, FBIS renders personal and place-names in accordance with the romanization systems approved for U.S. Government publications by the U.S. Board of Geographic Names.

Headlines, editorial reports, and material enclosed in brackets [] are supplied by FBIS/JPRS. Processing indicators such as [Text] or [Excerpts] in the first line of each item indicate how the information was processed from the original. Unfamiliar names rendered phonetically are enclosed in parentheses. Words or names preceded by a question mark and enclosed in parentheses were not clear from the original source but have been supplied as appropriate to the context. Other unattributed parenthetical notes within the body of an item originate with the source. Times within items are as given by the source. Passages in boldface or italics are as published.

SUBSCRIPTION/PROCUREMENT INFORMATION

The FBIS DAILY REPORT contains current news and information and is published Monday through Friday in eight volumes: China, East Europe, Soviet Union, East Asia, Near East & South Asia, Sub-Saharan Africa, Latin America, and West Europe. Supplements to the DAILY REPORTs may also be available periodically and will be distributed to regular DAILY REPORT subscribers. JPRS publications, which include approximately 50 regional, worldwide, and topical reports, generally contain less time-sensitive information and are published periodically.

Current DAILY REPORTs and JPRS publications are listed in *Government Reports Announcements* issued semimonthly by the National Technical Information Service (NTIS), 5285 Port Royal Road, Springfield, Virginia 22161 and the *Monthly Catalog of U.S. Government Publications* issued by the Superintendent of Documents, U.S. Government Printing Office, Washington, D.C. 20402.

The public may subscribe to either hardcover or microfiche versions of the DAILY REPORTs and JPRS publications through NTIS at the above address or by calling (703) 487-4630. Subscription rates will be

provided by NTIS upon request. Subscriptions are available outside the United States from NTIS or appointed foreign dealers. New subscribers should expect a 30-day delay in receipt of the first issue.

U.S. Government offices may obtain subscriptions to the DAILY REPORTs or JPRS publications (hardcover or microfiche) at no charge through their sponsoring organizations. For additional information or assistance, call FBIS, (202) 338-6735, or write to P.O. Box 2604, Washington, D.C. 20013. Department of Defense consumers are required to submit requests through appropriate command validation channels to DIA, RTS-2C, Washington, D.C. 20301. (Telephone: (202) 373-3771, Autovon: 243-3771.)

Back issues or single copies of the DAILY REPORTs and JPRS publications are not available. Both the DAILY REPORTs and the JPRS publications are on file for public reference at the Library of Congress and at many Federal Depository Libraries. Reference copies may also be seen at many public and university libraries throughout the United States.